



UNIVERSITY OF LEEDS

This is a repository copy of *Hydrogen production from simple alkanes and oxygenated hydrocarbons over ceria-zirconia supported catalysts: Review*.

White Rose Research Online URL for this paper:
<http://eprints.whiterose.ac.uk/90814/>

Version: Accepted Version

Article:

Nahar, G and Dupont, V (2014) Hydrogen production from simple alkanes and oxygenated hydrocarbons over ceria-zirconia supported catalysts: Review. *Renewable and Sustainable Energy Reviews*, 32. pp. 777-796. ISSN 1364-0321

<https://doi.org/10.1016/j.rser.2013.12.040>

© 2014, Elsevier. Licensed under the Creative Commons Attribution-NonCommercial-NoDerivatives 4.0 International
<http://creativecommons.org/licenses/by-nc-nd/4.0/>

Reuse

Unless indicated otherwise, fulltext items are protected by copyright with all rights reserved. The copyright exception in section 29 of the Copyright, Designs and Patents Act 1988 allows the making of a single copy solely for the purpose of non-commercial research or private study within the limits of fair dealing. The publisher or other rights-holder may allow further reproduction and re-use of this version - refer to the White Rose Research Online record for this item. Where records identify the publisher as the copyright holder, users can verify any specific terms of use on the publisher's website.

Takedown

If you consider content in White Rose Research Online to be in breach of UK law, please notify us by emailing eprints@whiterose.ac.uk including the URL of the record and the reason for the withdrawal request.



eprints@whiterose.ac.uk
<https://eprints.whiterose.ac.uk/>

Hydrogen production from simple alkanes and oxygenated hydrocarbons over ceria–zirconia supported catalysts: Review

Published in **Renewable and Sustainable Energy Reviews** (2014) 32:777-796.

Gaurav Nahar

gauravnahar@defiantenergy.in (updated email since publication)

Valerie Dupont

V.Dupont@leeds.ac.uk

Energy Research Institute, School of Chemical and Process Engineering, The University of Leeds, Leeds LS2 9JT, UK

Abstract

The use of ceria–zirconia based catalysts in hydrogen production from simple alkanes and oxygenated hydrocarbons for the processes of steam reforming (SR), autothermal reforming ('ATR'), catalytic partial oxidation ('CPO'), and dry reforming ('DR') are reviewed in this paper. Along with preparation methods, the effects of operating conditions like molar steam to carbon ratio, oxygen to carbon ratio, and temperature on the performance of hydrogen production from methane, acetic acid, ethanol, and glycerol were examined. SR and ATR of these feedstocks over ceria–zirconia supports have been widely investigated. In comparison the utilization of these supports in the CPO and DR processes has been investigated mainly for methane as compared to oxygenated hydrocarbons. Ce-rich supports were reported to be effective in hydrogen from SR and ATR of ethanol and glycerol and in SMR in the 'low' temperature range (500–600 °C), whereas zirconium-rich supports exhibited higher catalytic activity in the 'high' temperature range (700–800 °C). In the case of DR, Ce-rich supports were effective at high temperature.

The methods of preparation of the supports/catalyst are shown to affect the surface area (catalyst/support), crystallite size of (active metal/support), reducibility and dispersion of the active metal, thus affecting performance of the catalyst.

Abbreviations: ACCP, ammonium carbonate co-precipitation; AMCP, ammonia co-precipitation; AHCP, ammonium hydroxide co-precipitation; ATR, autothermal reforming; ATRE, autothermal reforming of ethanol; ATRM, autothermal reforming of methane; C, catalyst; CP, co-precipitation; CPOM, catalytic partial oxidation of methane; CPOE, catalytic partial oxidation of ethanol; DR, dry reforming; DRM, dry reforming of methane; HRTEM, high resolution transmission electron microscopy; IMP, impregnation; ME, micro-emulsion; MS, molten salt; MSSG, molten salt sol gel; OSC, oxygen storage capacity; PD, precipitation digestion; PFA, palm fatty acids; PFAD, palm fatty acid distillate; PH, potassium hydroxide; PHCP, potassium hydroxide co-precipitation; PHPP, potassium hydroxide precipitation; RME, reverse micro-emulsion; S, support; SA, surfactant assisted; SACP, surfactant assisted co-precipitation; SG, sol gel; SIMP, sequential impregnated; SCCP, sodium carbonate coprecipitation; SHCP, sodium hydroxide co-precipitation; SMR, steam methane reforming; SR, steam reforming; SRA, steam reforming of acetic acid; SRE, steam reforming of ethanol; SRG, steam reforming of glycerol; TEM, transmission electron microscopy; UC, urea combustion; UH, urea hydrolysis

Keywords: Hydrogen; Ceria–zirconia; Steam reforming; Autothermal reforming; Partial oxidation; Dry reforming

1 Introduction

Ceria based materials have attracted serious attention for utilization in automotive exhaust catalyst, ceramics, fuel cell technologies, gas sensors, solid state electrolytes, and ceramic biomaterials [1–6]. Ceria is an effective material in promoting reactions of catalytic carbon dioxide activation, carbon monoxide oxidation, carbon monoxide/nitrous oxide removal, and catalytic combustion of methane [7,8]. Ceria plays an important role in most important commercial catalytic processes like fluid catalytic cracking (FCC) [1], diesel soot oxidation [9], and oxidation of volatile organic compounds [10]. One of the crucial property of a ceria based material is its oxygen storage capacity (OSC) by means of redox shift between Ce^{3+} and Ce^{4+} under oxidizing and reduction environments [11]. Ceria exhibits superior catalytic activity for water gas shift reaction [12]. It is also well known to promote metal activity and dispersion, resulting in investigations of various catalytic formulations for a wide range of reactions.

The OSC of ceria helps to reduce the formation of carbon, over ceria supported catalyst during hydrogen production, methane oxidation, methane decomposition, and ethylene dehydrogenation reactions. Further, Ni supported ceria based catalysts have exhibited self-decoking capability by promoting carbon gasification reaction by supplementing oxygen species from the lattice oxygen. [13].

Hydrogen production from gaseous hydrocarbons like methane, ethane, propylene, butane, and liquefied petroleum gas (LPG) over ceria supported catalysts have been reported by Xu et al. [14], Pino et al. [15], Wang and Gorte [16], and Laosiripojana and Assabumrungrat [17]. Ceria supported catalysts were also reported to convert poisonous methanethiol (CH_3SH) to hydrogen-rich gas via the solid–gas reaction between ceria and methanethiol [18]. In the presence of steam, formation of $Ce(SO_4)_2$ was reported to occur during the steam reforming (SR) reaction leading to high methanethiol reforming activity. Likewise hydrogen production from liquid hydrocarbons like methanol, ethanol, glycerol and propanol were investigated by several authors [19–21]. However ceria lacks thermal stability and is known to sinter at temperature above 800 °C [22], leading to catalyst deactivation [23,24]. At high temperature the specific surface area of ceria decreases drastically which in turn affects the crucial redox properties and OSC of the material [25]. The OSC of pure ceria is unsatisfactory for practical applications. Ceria consists of eight oxygen anions coordinated at a corner of cube, each anion being tetrahedrally coordinated by four cations. This makes ceria's structure more stable and prevents the conversion of Ce^{4+} to Ce^{3+} under reducing conditions. Metal decoration has been observed for metal catalysts supported on reducible oxides [26]. Deterioration of catalytic activity is also caused by decreases in metal surface area on metal supported catalysts [27].

Hydrogen production from gases like methane using endothermic SR process is carried out at high temperature i.e. 800 °C or higher, resulting in decrease in surface area by ~30% with operation for 10 h [23]. Similarly the increase in the temperature of the ceria supported catalyst as a result of exothermic nature of partial oxidation reaction results in sintering of the ceria and affecting activity of the catalyst.

Improvement of the thermal properties of ceria and retention of active surface area at high temperature is thus necessary to exploit the redox property of ceria for hydrogen production applications via high temperature processes like catalytic partial oxidation ('CPO'). Substitution of ceria with metal/metal oxide into the ceria lattice forms composite oxides. Ceria can easily form solid solutions with elements belonging to the transition-metal series. Ionic mobility is modified by replacement of cerium ions by different cations of varying size and/or charge resulting in the formation of a defective fluorite structured solid solution. The crystal structure of $\text{Ce}_{0.75}\text{Zr}_{0.25}\text{O}_2$ obtained by zirconium doped ceria is shown in Fig. 1.

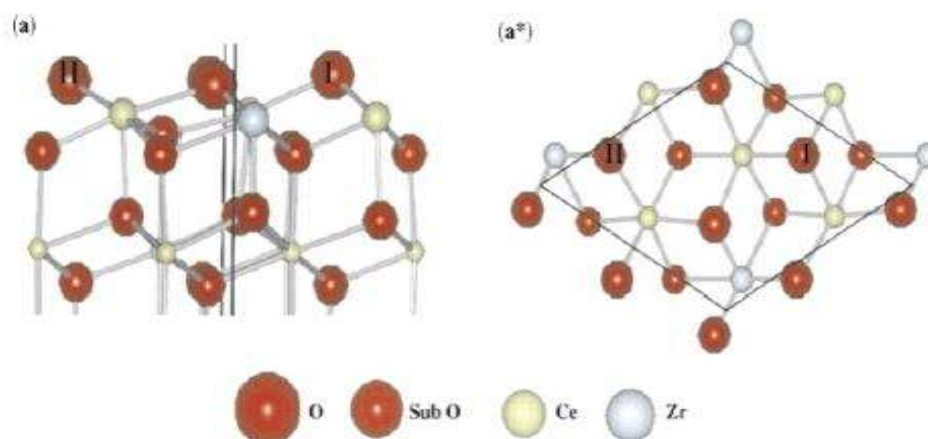


Fig. 1 Crystal structure of $\text{Ce}_{0.75}\text{Zr}_{0.25}\text{O}_2$. In (a) shows the side view and (a*) represents the top view of the $\text{Ce}_{0.75}\text{Zr}_{0.25}\text{O}_2$. The labels 'I' and 'II' represent two types of surface oxygen ions; the big red, small red, yellow, and blue shows surface oxygen, subsurface oxygen, Ce, and Zr, respectively [28]. (For interpretation of the references to color in this figure, the reader is referred to the web version of this article.)

Fig. 2 shows a high resolution transmission electron microscopy (HRTEM) image of $\text{Ce}_{0.75}\text{Zr}_{0.25}\text{O}_2$ prepared using the decomposition and co-precipitation method [29].

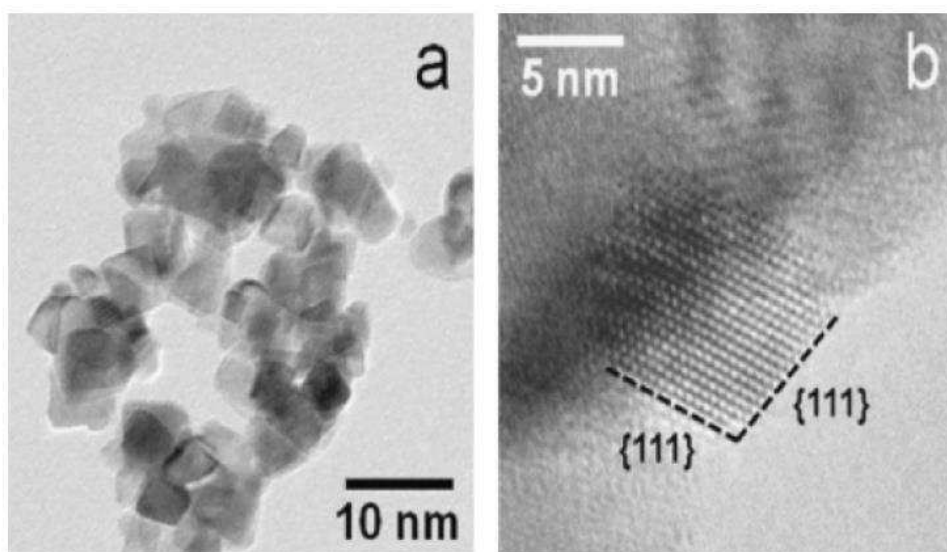


Fig. 2 HRTEM image of $\text{Ce}_{0.75}\text{Zr}_{0.25}\text{O}_2$ prepared using the decomposition and co-precipitation method calcined at $500\text{ }^\circ\text{C}$ [29].

This modification of ceria lattice confers properties like resistance to sintering and high catalytic activity [30–32]. Incorporation of Zr increases the specific surface area, OSC, redox property, thermal stability and catalytic activity of ceria [33–35]. It also affects the dispersion of metals supported on the Zr doped ceria. A transmission electron microscopy (TEM) image of dispersed Rh and Pt particles of fresh RhPt supported on 17.5 wt% CeO₂–ZrO₂ are shown in Fig. 3 [36].

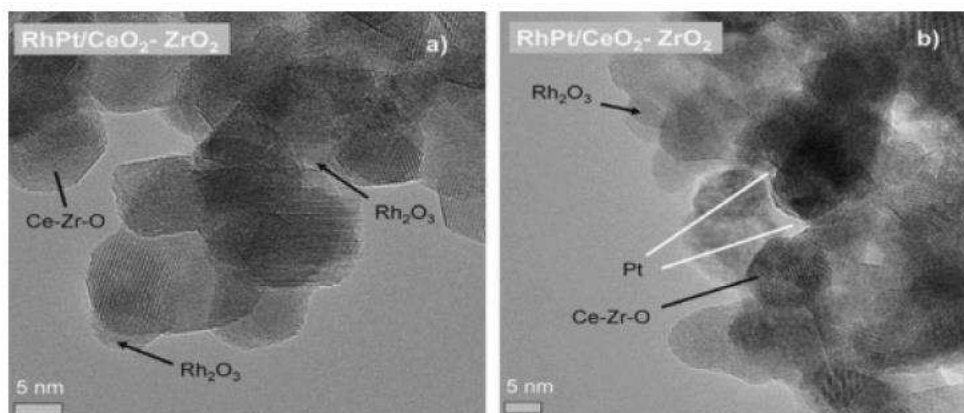


Fig. 3 TEM images of dispersed Rh and Pt particles of fresh RhPt supported on 17.5 wt% CeO₂–ZrO₂ catalyst [36].

Tables 1 and 2 show the effects of the preparation method on the surface area, OSC, and metallic dispersion of Ce–ZrO₂ supported metal catalysts utilized in hydrogen production processes. Further addition of Zr to Ce also helps in mitigating the formation of carbon during various hydrogen production processes [25]. Table 3 lists the amount of carbon deposited on various metals supported Ce–ZrO₂ catalysts prepared by varied methods, utilized in hydrogen production processes.

Table 1 Effect of preparation methods on the physicochemical properties of Ce-ZrO₂ supported catalysts utilized in hydrogen production.

Authors	Investigation	Support	Active metals	Method of preparation	Surface area m ² /g	Support size (nm)	Active metal size (nm)
Roh et al. [47]	SMR	Ce _{0.8} Zr _{0.2} O ₂	15 wt% Ni	15 wt% Ni	168 ^b	5.2	
Roh et al. [62]	SFE	Ce _{0.2} Zr _{0.8} O ₂	2 wt% Rh	aq-AMCP	98 ^b		
Lin et al. [58]	SFE	Ce _{0.75} Zr _{0.25} O ₂	10 wt% Co	SHCP	92.5 ^b	4.5	
Jun et al. [119]	DRM	Ce _{0.9} Zr _{0.1} O ₂	15 wt% Ni	AMCP	92	5.9	12.5
Kusakabe et al. [45]	SMR	Ce _{0.5} Zr _{0.5} O ₂	10 wt% Ni	U H	81.1 ^a		
Roh et al. [61]	SFE	Ce _{0.8} Zr _{0.2} O ₂	2 wt% Rh	PHPD	61		
Dong et al. [49]	SMR	Ce _{0.2} Zr _{0.8} O ₂	15 wt% Ni	M S	55 ^a		112
Roh et al. [60]	SFE	Ce _{0.13} Zr _{0.87} O ₂	1 wt% Rh	Commercial	44 ^a		
					44 ^b		
Shotpruk et al. [56]	SR of PEAD	Ce _{0.75} Zr _{0.25} O ₂	5 wt% Ni	SA-aq-AMCP	46.5 ^a		
Laostripojana et al. [24]	SMR	Ce _{0.75} Zr _{0.25} O ₂	5 wt% Ni	SA-aq-AMCP	41.5 ^a		
			5 wt% Rh		19.5 ^b		
					40.9 ^b		
Laostripojana et al. [55]	SR of PEAD						
Roh et al. [48]	SMR	Ce _{0.2} Zr _{0.8} O ₂	15wt %Ni	SG	44 ^b		12.7
Roh et al. [46]	SMR	Ce _{0.2} Zr _{0.8} O ₂	15wt %Ni	S G	40 ^b		
Biswas and Kunzru [19]	SFE	Ce _{0.74} Zr _{0.26} O ₂	30 wt% Ni	aq-AMCP	22.8 ^a	12.5	17.3
					19.5 ^b		
Dave and Pant [21]	SRG	CeO ₂ /10 wt% ZrO ₂	15 wt% Ni	IMP	22 ^b		
Hu et al. [67]	SFA	5 wt% CeO ₂ -ZrO ₂	5 wt% Ni	AHCP	20.6 ^b		
Zheng et al. [66]	SFA	7.5 wt% CeO ₂ -ZrO ₂	12 wt% Ni	IMP	14.61 ^b		

^a Support.

^b Catalyst.

Table 2 Effect of preparation methods on OSC and metal dispersion of metal supported on Ce-ZrO₂ catalysts, utilized in hydrogen production.

Author	Investigation	Method of preparation	Catalyst/support	Reported OSC value:hydrogen uptake (μmol/gcat)	Metallic dispersion (%)
Silva et al. [85]	POM	IMP	0.5 wt%Pt-Ce _{0.75} Zr _{0.25} O ₂ -Al ₂ O ₃	246 ^b	100
			1.0 wt%Pt-Ce _{0.5} Zr _{0.5} O ₂ -Al ₂ O ₃	245 ^b	77
			1.5wt %Pt-Ce _{0.25} Zr _{0.75} O ₂ -Al ₂ O ₃	242 ^b	57
			1.5 wt% Pt/40% Ce _{0.6} Zr _{0.4} O ₂ /Al ₂ O ₃	783 ^b	68
			1.5 wt% Pt/20% Ce _{0.6} Zr _{0.4} O ₂ /Al ₂ O ₃	483 ^b	64
			1.5 wt% Pt/10% Ce _{0.6} Zr _{0.4} O ₂ /Al ₂ O ₃	291 ^b	58
Silva et al. [96]			1.5 wt% Pt/30% Ce _{0.6} Zr _{0.4} O ₂ /Al ₂ O ₃	588 ^b	57
Silva et al. [95]	POM	Co-IMP	1.5 wt%Ni-Ce _{0.25} Zr _{0.75} O ₂ -Al ₂ O ₃	115 ^b	54
			1.5 wt%Ni-Ce _{0.5} Zr _{0.5} O ₂ -Al ₂ O ₃	565 ^b	49

Siva et al. [94]				1.5 wt%Pt-Ce _{0.7} Zr _{0.2} O ₂ -Al ₂ O ₃	215 ^a	47
				1.5 wt%Pt-Ce _{0.7} Zr _{0.2} O ₂ -Al ₂ O ₃ -pp	215 ^b	42
Roh et al. [62]	SRE	aq-AMCP		2 wt%-Rh-Ce _{0.8} Zr _{0.2} O ₂	-	46.3
Roh et al. [60]		IMP		1 wt%-Rh-Ce _{0.8} Zr _{0.18} O ₂		
Boulois-Eras et al. [99]	POM	IMP		0.5 wt%Ni-Ce _{0.7} Zr _{0.3} O ₂ -Al ₂ O ₃	-	41
				0.5 wt%Ni-Ce _{0.25} Zr _{0.75} O ₂ -Al ₂ O ₃	-	38
Ruiz et al. [72]	ATRM	AHCP		1.5 wt%Pt-Ce _{0.7} Zr _{0.2} O ₂ -800	626 ^a	22
				1.5 wt%Pt-Ce _{0.7} Zr _{0.2} O ₂ -900	726 ^a	11
Roh et al. [47]	Combined methane reforming	PHCP		5 w % Ni-Ce _{0.8} Zr _{0.2} O ₂	-	7.96
Roh et al. [48]	SMR					6.60
Roh et al. [50]	SMR	IMP		15 wt%Ni-Ce _{0.2} Zr _{0.8} O ₂ -Al ₂ O ₃	42.85 ^b	4.99
				12 wt%Ni-Ce _{0.2} Zr _{0.8} O ₂ -Al ₂ O ₃	32.80 ^b	4.96
				6 wt%Ni-Ce _{0.2} Zr _{0.8} O ₂ -Al ₂ O ₃	13.50 ^b	4.70
				3 wt%Ni-Ce _{0.2} Zr _{0.8} O ₂ -Al ₂ O ₃	5.38 ^b	3.53
Laosiripojana et al. [55]	SR of PFAD	SA-aq-AMCP		5 wt%-Rh-Ce _{0.7} Zr _{0.25} O ₂	-	4.62
Kumar et al. [123]	DRM	SA-aq-AMCP		5 wt%-Ni-Ce _{0.8} Zr _{0.4} O ₂	-	4.30
Dong et al. [49]	SMR	SG		10 w % Ni-Ce _{0.2} Zr _{0.8} O ₂	7.32	1.05
					7.32 ^b	0.86
				15 w % Ni-Ce _{0.2} Zr _{0.8} O ₂	11.5 ^b	0.74
					98.8 ^b	0.41
				20 wt%-Ni-Ce _{0.2} Zr _{0.8} O ₂	0.799 ^b	0.48
				3 wt%-Ni-Ce _{0.2} Zr _{0.8} O ₂		
Roh et al. [68]	SMR	SG		3 wt%-Ni-Ce _{0.2} Zr _{0.8} O ₂	228.8 ^a	0.86
				15 wt%-Ni-Ce _{0.2} Zr _{0.8} O ₂	214.9 ^a	
Roh et al. [46]				15 wt%-Ni-Ce _{0.2} Zr _{0.8} O ₂	9.39 ^a	
Liébois et al. [73]	ATRM	AHCP		10 wt%Ni-Ce _{0.7} Zr _{0.25} O ₂	551 ^a	0.68
Biswas and Kunzru [19]	SRE	aq-AMCP		20 wt%Ni-Ce _{0.34} Zr _{0.25} O ₂	7.14 ^b	0.42
				30 wt%Ni-Ce _{0.74} Zr _{0.35} O ₂	7.60 ^b	0.30
				30 wt%Ni-Ce _{0.34} Zr _{0.25} O ₂	2.03 ^b	0.24

				40 wt% Ni-Ce _{0.3} Zr _{0.3} O ₂	6.27 ^a	0.19
Chen et al. [115]	DRM	AMCP		0.5 wt% Ru-Ce _{0.75} Zr _{0.25} O ₂	0.7 ^c	-
				1 wt% Ru-Ce _{0.75} Zr _{0.25} O ₂	1.1 ^c	
				1.5 wt% Ru-Ce _{0.75} Zr _{0.25} O ₂	8.9 ^c	
				3 wt% Ru-Ce _{0.75} Zr _{0.25} O ₂	14.5 ^c	
Damyanova et al. [114]	DRM	IMP		1 wt% Pt-1 wt% CeO ₂ -ZrO ₂	0.51	-
				1 wt% Pt-3 wt% CeO ₂ -ZrO ₂	0.57	
				1 wt% Pt-6 wt% CeO ₂ -ZrO ₂	0.62	
				1 wt% Pt-12 wt% CeO ₂ -ZrO ₂	1.25	
Quingwei et al. [100]	POM	PP Mixing PP Mechanically mixing		10 wt% Ni-Ce _{0.3} Zr _{0.3} O ₂ -Al ₂ O ₃	-	1.16
				10 wt% Ni-Ce _{0.3} Zr _{0.3} O ₂ -Al ₂ O ₃		0.75
				10 wt% Ni-Ce _{0.3} Zr _{0.3} O ₂ -Al ₂ O ₃		0.46
Shodpruk et al. [56]	SR of PFAD	SA-aq-AMCP		5 wt% Ni-Ce _{0.75} Zr _{0.25} O ₂	5313 ^b	-
Sukoniet et al. [124]	DRM	SA-aq-AMCP		Ce _{0.8} Zr _{0.4} O ₂ -1.25	1093	-
				Ce _{0.8} Zr _{0.4} O ₂ -0.8	1031	
				Ce _{0.8} Zr _{0.4} O ₂ -0.5	93	

^a Support.

^b Catalyst.

Table 3 Effect of preparation methods on reducibility of metal supported on Ce-ZrO₂ catalysts utilized in hydrogen production.

Authors	Investigation	Preparation method	Catalyst/support	Metal reducibility (%)
Blewas and Kunzru [19]	SFE	aq-AMCP	10% Ni/Ce _{0.7} Zr _{0.3} O ₂	97.3
Atreu et al. [51]	SMR	ACCP	5 wt% Ni-Ce _{0.7} Zr _{0.3} O ₂ -Al ₂ O ₃	96.4
Roh et al. [50]	SMR	IMP	15 wt% Ni-Ce _{0.7} Zr _{0.3} O ₂ -Al ₂ O ₃	92.3
Loasripojana et al. [55]	SR of PFAD	aq-AMCP	5 wt% Rh-Ce _{0.7} Zr _{0.3} O ₂	92
Roh et al. [48]	Combined methane	aq-AMCP	15 wt% Ni-Ce _{0.7} Zr _{0.3} O ₂	53.7
Roh et al. [47]	Reforming SMR	aq-AMCP	15 wt% Ni-Ce _{0.7} Zr _{0.3} O ₂	40.8

Table 4 Effect of preparation methods on carbon production on metal supported Ce-ZrO₂ catalysis utilized in hydrogen production.

Authors	Investigation	Preparation method	Catalyst/support	C
Jun et al. [119]	DRM	CP	15 wt%Ni-Ce _{0.5} Zr _{0.2} O ₂	<0.0001 g _c g _c ⁻¹
Abreu et al. [51]	SMR	ACCP	5 wt%Ni-Ce _{0.6} Zr _{0.4} O ₂ -Al ₂ O ₃	0.34 mmol h ⁻¹ ^a
Vagia and Lemonidou [65]	SRA	IMP	5 wt% Ni-Ce _{0.88} Zr _{0.12} O ₂	1.5 wt% of catalyst ^b
			0.5 wt% Rh-Ce _{0.88} Zr _{0.12} O ₂	0.5 wt% of catalyst ^b
Laosiripojana et al. [108]	PO of PFAD	aq-AMCP	5 wt%Ni-Ce _{0.75} Zr _{0.25} O ₂	3.9 mmol C g _c cat ⁻¹
Kamonsungkasem et al. [80]	ATR	IMP	5% wt% Ni(8%CeO ₂ -ZrO ₂ -Al ₂ O ₃)	4.4 mmolC g _c cat ⁻¹ h ⁻¹ , S/C=1 ^c
				4.3 mmolC g _c cat ⁻¹ h ⁻¹ , S/C=2 ^c
				4.2 mmolC g _c cat ⁻¹ h ⁻¹ , S/C=3 ^c
Shoibruk et al. [56]	SR of PFAD ATR of PFAD	aq-AMCP	5 wt%Ni-Ce _{0.75} Zr _{0.25} O ₂	5.1 mmol g _c cat ⁻¹ d 3.9 mmol g _c cat ⁻¹ d
Laosiripojana et al. [55]	SR of PFAD ATR of PFAD	aq-AMCP	5 wt%Rh-Ce _{0.75} Zr _{0.25} O ₂	10 mmol C g _c cat ⁻¹ ^b 3.5 mmol C g _c cat ⁻¹ ^b
Qingwei et al. [100]	POM	CP with mixing CP Mechanical mixing	10 wt%NiCe _{0.75} Zr _{0.25} O ₂ /γ-Al ₂ O ₃	19.2 14.7 7.1

^a Catalyst was evaluated for 350 min at 750 °C at S/C of 2.

^b The performance of the catalyst was evaluated at 900 °C at S/C of 3 for 10 h. The ATR evaluation was performed using O₂/C of 1.

^c The performance of the catalyst was evaluated at 800 °C at S/C of 3 for 48 h. The PO and ATR experiments were performed using O₂/C of 1.

^d The catalyst performance was evaluated at O₂/C of 0.15 at 550 °C.

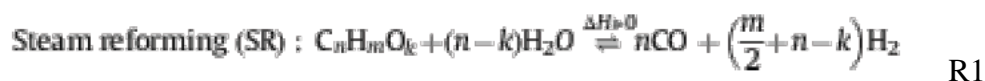
^e The catalyst was evaluated for 3 h at 750 °C at S/C of 3.

The inclusion of Zr⁴⁺ or Hf⁴⁺ into ceria lattice facilitated an increase in the formation of smaller particle sizes. In addition, incorporation of Zr also increases the oxygen mobility in the ceria lattice and the process of vacancy formation, thus increasing the reducibility of the material [33,37,38]. This extends ceria reduction deep into the bulk of the material, rather than confining to the surface [34,39]. Addition of Zr increases the interactions between the support and the metal. During the reductive treatment, transfer of Ce⁴⁺ to the support surface takes place, resulting in the formation of ceria-rich phase on the surface while the phenomenon is reversed when atmosphere was switched to an oxidative atmosphere [40]. Fig. 4 shows a migration model of Ce⁴⁺ and oxygen vacancies during the reductive/oxidative treatments of ceria–zirconia mixed oxide [40]. An oxidation treatment was shown to increase the reducibility of the oxide. In case of Pt supported on ceria–zirconia mixed oxide, Pt sites and the Ce Pt located at the interface interact, and transfer of electrons from the metal oxide to the noble metal occurs. This results in the lowering of effective activation energy, necessary for the formation of oxygen vacancies, resulting in high oxidation activity [40,41]. Fig. 5 shows a shell–core structure of Pt crystallites and the decoration/encapsulation by ceria–zirconia support during the reductive/oxidative treatments [40]. The percentage of reducible Ce⁴⁺ is known to increase with Zr/Ce ratio. The effect of preparation methods on the reducibility of metal supported Ce–ZrO₂ catalyst used in hydrogen production processes is shown in Table 3.

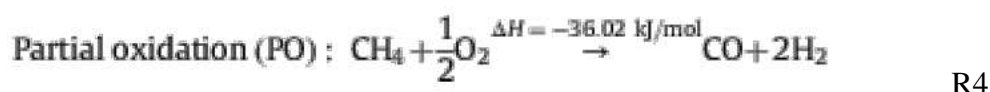
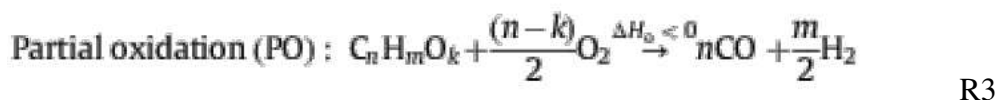
This review examines the application of ceria based material in hydrogen production from simple alkanes and oxygenated hydrocarbons using various processes. Methods of preparation, operating conditions and performance of the catalyst in terms of hydrogen yield, selectivity, molar composition and fuel conversion are also investigated.

2 Hydrogen production

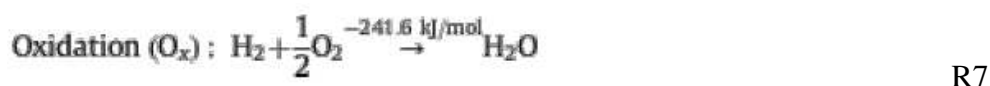
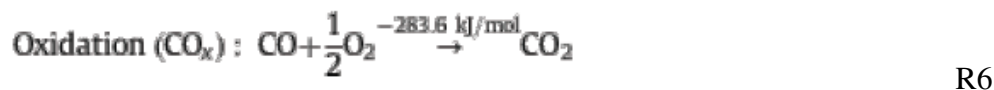
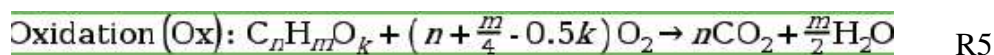
Several processes to produce hydrogen-rich gas for fuel cell applications are being employed today. Hydrogen can be produced using catalytic steam reforming ('SR'), catalytic partial oxidation ('CPO'), autothermal reforming ('ATR'), and CO₂ reforming of methane, which is also known as dry reforming ('DR'). SR is the most common process used to produce hydrogen in industry. Hydrocarbon fuel is reacted with steam at high temperature around 800 °C. The reaction is performed in tubular packed bed reactors called reformers on Ni based catalyst in Raschig rings using a molar H₂O/CH₄ ratio typically between 2 and 5, but most often around 2.5. Alkali metals are used in the catalyst to accelerate carbon removal. Excess steam is used to prevent carbon formation. SR reaction is strongly endothermic, and reactor designs are typically limited by heat transfer, rather than by reaction kinetics [42]. The general SR reaction is represented by R-1 and R-2 explains steam methane reforming ('SMR').



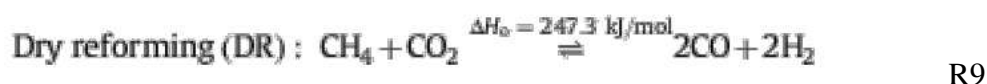
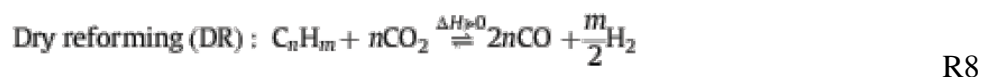
Partial oxidation ('PO') is exothermic reaction. If higher oxygen is fed, combustion reaction also occurs, resulting in the formation of carbon dioxide and steam rather than carbon monoxide and hydrogen. In addition PO is kinetically faster than SR and requires smaller reactors and exhibits higher productivity [43]. A major drawback of PO is the formation of flammable and explosive environments. Hot spots can develop affecting the life of the catalyst [44]. Reaction R-3 represents a generic reaction for the PO of oxygenated hydrocarbons. The PO of methane is given by reaction R-4.



Autothermal reforming (ATR) is a combination of SR and CPO reactions. The method uses exothermic heat of the oxidation reactions to provide the heat required by the endothermic reforming reaction in a single unit to produce hydrogen-rich gas. The method is useful for small scale hydrogen production because of faster start up, small size, higher efficiency, fuel flexibility and hydrogen purity. Reactions R-1 and R-3 take place in ATR along with the complete oxidation reaction R-5, which includes the reactions R-6 to R-7.

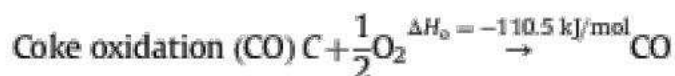
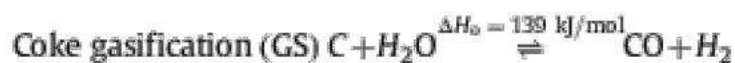
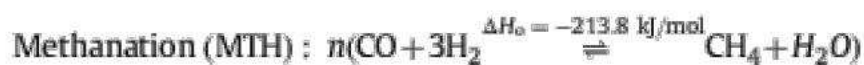
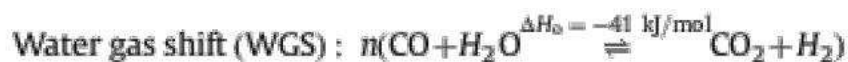


In addition to the above hydrogen production methods, CO₂-reforming of methane, also termed 'dry reforming' (DR) has recently received some interest as reforming method because of its carbon dioxide recycling potential. In this method the fuel is reacted with carbon dioxide to form syngas. In case of dry reforming synthesis gas having H₂/CO ratio of 1 is produced making it suitable for F-T synthesis. Reaction R-8 shows the general case where a hydrocarbon undergoes dry-reforming, with R-9 representing the dry reforming of methane.



DRM is the most endothermic of the reforming reactions due to the large negative enthalpy of CO₂. Side reactions like water gas shift (R-10), methanation (R-11), carbon formation (R-12), carbon monoxide disproportionation (Boudouard reaction

(R-13)), gasification reaction (R-14), and oxidation reactions (R15–16) can take place on the catalyst surface, affecting the performance of the above mentioned processes.



(R10 to R16)

2.1 Steam reforming

Ce–ZrO₂ supported catalysts have been widely investigated in hydrogen production via SR, CPO, ATR, and WGS reactions. The following section describes the use of various ceria–zirconia supported catalysts in SR of alkanes and oxygenated hydrocarbons.

2.1.1 Steam methane reforming (SMR)

Kusakabe et al. [45] examined the effect of noble metals supported on Ce–ZrO₂ material prepared by urea hydrolysis ('UH'), for SMR in the temperature range 500–600 °C using a molar steam to carbon ratio ('S/C') of 2. Over Pt and Rh supported catalyst the conversion increased with loading from 1 to 3 wt% but further loading lowered conversion. Contradictorily in case of Ru based catalyst conversion improved with loading, in the entire range examined (1 to 5 wt%). The authors reported that a cubic structure based mix oxide (Ce_{0.5}Zr_{0.5}O₂) exhibited higher activity in comparison to (Ce_{0.75}Zr_{0.25}O₂) supports, contrary to Laosiripojana et al. [24], who found that Ce_{0.75}Zr_{0.25}O₂ exhibited higher activity than other phases of Ce–ZrO₂ supports in SMR. Carbon monoxide selectivity was higher over noble metals in comparison to Ni based catalyst possibly as a result of dehydrogenation of methane. SMR over 5 wt%-Ni/Ce–ZrO₂ at 900 °C was examined by Laosiripojana and Assabumrungrat [23] using S/C of 3. The support was prepared by UH of metal salts by varying the molar ratio of Ce to Zr ('Ce/Zr') from 1 to 3. Ce_{0.75}Zr_{0.25}O₂ exhibited the best performance among the catalysts examined. The support prepared using this method had lower surface area as compared to the supports prepared using the ammonia co-precipitation ('AMCP') method [24]. The authors examined the effect of surfactant addition in the support

preparation method which involved AMCP of cerium and zirconium nitrate salts. Addition of surfactant considerably increased the support surface area.

In spite of higher catalytic activity slight deactivation due to the sintering of material was reported. The addition of the surfactant was also shown to affect the dispersion of the Ni [24]. At odds with these results Roh et al. [46] reported similar results over 15 wt% Ni supported on Ce_{0.2}Zr_{0.8}O₂ prepared by the molten salt method ('MS') at 750 °C using S/C of 3.

Roh et al. [47] examined low temperature SMR over Ni supported on potassium hydroxide precipitation ('PHPP') Ce–ZrO₂ supports. The effect of Ce/Zr on the performance of the catalyst was evaluated using 10 wt% Ni loading at 600 °C and S/C of 1, with Ce_{0.8}Zr_{0.2}O₂ exhibiting the best performance. The higher activity of the catalyst was attributed to higher thermal stability, higher redox capability of Ce–ZrO₂, smaller Ni crystallite size resulting in higher carbon resistance, cubic phase of the support improving the reducibility and thus helping in the reduction of metal sintering.

Roh et al. [48] compared the impregnation ('IMP') and co-precipitation ('CP') methods for preparation of 15 wt% Ni supported Ce_{0.8}Zr_{0.2}O₂ catalyst in SMR with small amount of carbon dioxide. The activity of Ce–ZrO₂ based catalysts using S/C ratio of 1 and CH₄/CO₂ of 0.5 was examined between 700 and 800 °C. The Ni Ce ZrO₂ catalyst prepared by the CP method was found more effective as compared to the conventional IMP catalyst. Highest activity as well as stability of the CP catalyst was attributed to nano-sized crystallite of both Ce_{0.8}Zr_{0.2}O₂ and NiO resulting in the formation of intimate contact between Ni and the support, improved Ni dispersion, and finally enhanced reducibility and oxygen transfer during the reaction. Smaller crystallite size of support and NiO was reported over the CP catalyst in comparison to the impregnated ones. Ni dispersion and surface area were quite high over the CP catalyst compared as to the impregnated ones. Effect of Ni loading on the performance of sol gel ('SG') prepared Ce_{0.8}Zr_{0.2}O₂ supported catalyst in SMR at 750 °C and S/C of 3 was examined by Dong et al. [49]. Ni surface area and hydrogen uptake were reported to increase with loading from 3% to 20% and upon further increase in loading they decreased, which was attributed to sintering of Ni particles. The activity of the catalyst was related to the dispersion of the catalyst and Ni surface area. Higher loading catalyst exhibited higher average crystallite sizes, promoting carbon formation. The high activity of the catalyst was mainly as a result of good balance between two kinds of active sites, i.e. one for the activation of methane and the other for that of steam or oxygen.

In comparison to Ni impregnated Ce_{0.8}Zr_{0.2}O₂ catalyst, Ni/Ce_{0.2}Zr_{0.8}O₂/θ-Al₂O₃ catalyst prepared by the IMP method exhibited better performance in SMR at 800 °C with S/C of 1 [50]. The high stability of the catalyst was mainly ascribed to the beneficial pre-coating effect of Ce–ZrO₂ which resulted in the formation of stable NiO_x species, a strong interaction between Ni and the support, an abundance of mobile oxygen species, resulting in high carbon resistance. Authors reported that methane conversion increased with Ni loading from 3 to 12 wt% but further increases reduced conversion. Abreu et al. [51] reported dissimilar results over 5 wt% Ni supported on Ce_{0.2}Zr_{0.8}O₂-γ-Al₂O₃ catalyst in SMR, prepared using the ammonium hydroxide coprecipitation ('AHCP') method at S/C of 2.1 and 750 °C. Although the Zr-rich catalyst initially exhibited higher conversion, it underwent severe deactivation with time on stream. The catalyst with higher Ce content was reported to help in the reduction of Ni species, which otherwise resulted in increased methane decomposition to form carbon. But the presence of Ce favoured the activation of steam resulting in carbon gasification, leading to a stable catalytic formulation.

2.1.2 Steam reforming of methanol (SRMe)

Like methane, Ce–ZrO₂ has been investigated widely in ethanol ('SRE') [19,52,53], glycerol ('SRG') [21], bio-oils [54], and complex oxygenated hydrocarbons like palm oil fatty acid ('PFAD') [55,56]. But Ce–ZrO₂ has not been investigated widely in SR of methanol ('SRMe') [20,57], the motive of the investigations was to utilize this support to produce high purity hydrogen and prevent the formation carbon monoxide using oxygen vacancies from the support. The use of 8 wt% Cu supported on CeO₂/ZrO₂ at 250 °C was investigated by Oguchi et al. [57]. During the SR reaction CuO was reduced to metallic Cu, which, although it exhibited high activity for SRMe, it suffered sintering of crystallites. Addition of Zr leads to the formation of Cu₂O rather than CuO.

Presence of Cu₂O was shown to affect the durability of the catalyst by being less reducible to metallic Cu, during the SR reaction. Addition of Zr maintained the formation of Cu₂O under the reducing environment in SRMe conditions, by providing an oxygen source (OH) and maintaining the oxidation state of Cu. Further addition of Zr led to increase in Cu aggregation, and helped in the formation of smaller Cu₂O species than metallic Cu.

A 3 wt% Au supported Ce–ZrO₂ catalyst for SRMe was investigated by Pojanavaraphan et al. [20] in the temperature range of 200 to 500 °C using S/C of 2. The evaluation of different support compositions revealed Ce_{0.75}Zr_{0.25}O₂ to exhibit the best performance. The formulations with higher Zr content had a negative effect on the performance of the catalyst by increasing Au particle size. Two different support preparation methods i.e. sodium carbonate co-precipitation ('SCCP') and UH followed by IMP of Au salts were evaluated. Both the methods of preparation exhibited similar performance. The increase in pH up to 7 had a positive effect on the performance of CP catalyst. Addition of Cu to Au exhibited similar performance to Cu based catalyst.

Addition of Cu was shown to preserve the small alloy size and result in the formation of Au–Cu alloy thereby significantly promoting SRMe.

2.1.3 Steam reforming of ethanol (SRE)

SRE over Ni/Ce–ZrO₂ prepared by AMCP and incipient wetness IMP technique was investigated by Biswas and Kunzru [19] at S/C of 4 between 400 and 650 °C. A 30 wt% Ni supported on cubic phased Ce_{0.74}Zr_{0.26}O₂ support exhibited the best catalytic activity. Like Roh et al. [48] who reported the high activity of Ni/Ce_{0.8}Zr_{0.2}O₂ in SMR, they attributed high activity to the extent of reduction of Ni in the catalyst. Higher Ni loading up to a certain amount resulted in increase in reduced Ni enhancing the activity of the catalyst. High OSC capacity of the catalyst increased the availability of surface oxygen on the material, enhancing the WGS reaction, resulting in high activity. On the other hand Ye et al. [53] reported that a 20 wt% Ni catalyst supported on cubic Ce_{0.5}Zr_{0.5}O₂ exhibited high activity for SRE with S/C of 1.5 between 350 and 600 °C.

Unlike Ni supported catalyst, Co supported on cubic Ce_{0.75}Zr_{0.25}O₂ catalyst prepared by the IMP method exhibited higher activity in comparison to the supports prepared by the CP method, in SRE Lin et al. [58]. The activity of the catalyst was examined over 10 wt%-Co/Ce_{0.75}Zr_{0.25}O₂ with S/C of 6.5 at 450 °C. Under SR conditions a formation of unidentified active phase resulting from reaction between the partially reduced Co and Ce–ZrO₂ catalyst was reported to exhibit superior catalytic activity. The authors attributed the high activity of the catalyst to the reduction behavior of the catalyst like Biswas and Kunzru [19] and

Roh et al. [48]. A weaker contact between the active metal and support was seen, which was partially reduced during reduction of the catalyst.

Maia et al. [59] examined the use of 10 wt% Co/Ce_{0.8}Zr_{0.2}O₂ prepared by ethylene glycol and the citric acid polymerization method, in SRE. The activity of the catalyst was measured using S/C of 1.5 between 400 and 600 °C. High activity of the catalyst was found to be temperature dependent as a result of doping of Ce with Zr which yielded enhanced oxygen vacancies and redox capacity of the support to promote the oxidation of carbon monoxide. Higher activity of Co for WGS reaction was one of the factors responsible for increasing the activity of the catalyst at lower temperatures.

Roh et al. [60] described a 2 wt% Rh on cubic phased Ce_{0.13}Zr_{0.87}O₂ prepared by the IMP method exhibiting high catalytic activity in SRE. Similar to Ni based catalysts, strong interaction between Rh and the support play an important part in enhancing oxygen transfer efficiency during ethanol SR reactions. The catalyst promoted dehydrogenation or C–C cleavage of ethanol rather than dehydration, thus exhibiting high catalytic activity. In a different evaluation the increase in Zr in Rh supported on Ce–ZrO₂ decreased the activity of the catalyst in SRE [61]. Roh et al. [61] examined the effect of Ce/Zr ratio on performance of Rh based catalyst in SRE using S/C of 4 at 450 °C. They reported that the 2 wt% Rh supported on Ce_{0.2}Zr_{0.8}O₂ most severely deactivated among all the formulations studied, as a result of increased ethylene formation. Addition of 0.5% potassium ('PH') had a beneficial effect on catalyst stability, while higher potassium content (about 5%) lowered the catalytic activity. A Ce_{0.8}Zr_{0.2}O₂ support was the best formulation as a result of higher OSC, and strong interaction between Rh and Ce_{0.8}Zr_{0.2}O₂ had a positive effect on the performance of the catalyst reflected in an increased oxygen transfer efficiency [62]. The deactivation behavior of this formulation was studied by Platon et al. [44]. Addition of acetone and ethylene to the feed caused deactivation of 2 wt% Rh supported on Ce_{0.8}Zr_{0.2}O₂ prepared by the AMCP method, in SRE at 350 °C and S/C of 4. But the catalyst activity was recovered by addition of small amount of oxygen which regenerated the deactivated catalyst. A different reason for deactivation of 1.5 wt% Pt/Ce_{0.75}Zr_{0.25}O₂ in SRE was reported by de Lima et al. [63]. SRE was performed by the authors using S/C of 1.5 at 500 °C. Catalyst deactivation was attributed to acetate or carbonate species observed on the surface of the catalyst. The O₂ defects on ceria promoted activation of H₂O to OH groups. The OH groups reacted with carbon monoxide to produce formate molecule. Pt assisted the dehydrogenation of the formate molecule resulting in carbonate formation. Like Ye et al. [53], Birot et al. [64] reported high activity over 1 wt% Rh supported on commercial Ce_{0.5}Zr_{0.5}O₂ at 600 °C with S/C of 2. The catalyst had high selectivity to methane. Carbon monoxide and carbon dioxide hydrogenation over the catalyst was examined by the authors with CO/H₂ and CO₂/H₂ of 4 between 400 and 600 °C. The catalyst catalyzed carbon monoxide and carbon dioxide methanation reactions.

2.1.4 Steam reforming of oxygenated hydrocarbons

Similarly to Roh et al. [60], Vagia and Lemonidou [65] reported that 0.5 wt% Rh supported Ce_{0.86}Zr_{0.16}O₂ catalyst prepared by the IMP method exhibited high catalytic activity in steam reforming of acetic acid ('SRA'), used as a model component of biooil.

The activity was attributed to low affinity towards carbon formation and high oxygen mobility of Ce–ZrO₂ facilitating surface oxidation reactions to the metal interface leaving the surface of the catalyst clean. Yan et al. [54] gave accounts of similar results during SR of bio oil over sequential impregnated ('SIMP') of Ni and Ce over ZrO₂ prepared using the CP method to obtain a Ni/CeO₂–ZrO₂ catalyst.

Increase in temperature and Ni loading affected the catalytic activity. While increase in Ce loading along with S/C increased activity up to certain value, on further increase of S/C it decreased the activity. The catalyst exhibited higher catalytic activity compared to a commercial catalyst. The best performance was reported over 12 and 7.5 wt% Ni and Ce loading respectively, with water/bio oil ratio of 4.9 at 800 °C exhibiting highest hydrogen yield. Similarly Zheng et al. [66] examined the use of 12 wt% Ni supported on Ce–ZrO₂ catalyst obtained using the CP method, in SRA at 650 °C with S/C of 3. An optimum Ce content of 7.5 wt% was reported, similar to Yan et al. [54], but the optimum results were obtained at 650 °C in comparison to 800 °C. Higher temperatures i.e. 700 °C were reported to promote reverse WGS over the catalyst. At 600 °C and lower S/C of 1.5, Hu et al. [67], reported that 12 wt% Ni supported on Ce–ZrO₂ prepared using the CP method, with Ce content of 5 wt% deactivated as result of formation of acetone and carbon monoxide. Polymerization of acetone and carbon monoxide disproportionation reactions were reported responsible for catalyst deactivation. Higher temperature helped in preventing carbon formation from carbon monoxide disproportionation due to OSC of the material, but acetone polymerization was unaffected with rise in temperature.

Ni supported on cubic Ce_{0.75}Zr_{0.25}O₂ prepared by the surfactant assisted coprecipitation ('SACP') method was reported to exhibit high activity in SR of complex oxygenated hydrocarbons like palm fatty acid distilled ('PFAD') by Shotipruk et al. [56]. The catalyst performance was evaluated at 900 °C with S/C of 3. The catalyst provided the highest SR reactivity along with greatest carbon deposition resistance as a result of high OSC of this material. Also, comparison of model components of PFAD showed increase in the formation of ethylene with increase in degree of unsaturation from palmitic to linoleic acid, which meant increase in carbon content. But the degree of unsaturation also corresponded to a lower selectivity to hydrogen. High activity over 5 wt% Rh/Ce_{0.75}Zr_{0.25}O₂ at slightly lower temperature i.e. 800 °C at S/C of 3 over a support prepared by the same SACP method was reported by Laosiripojana et al. [55]. As compared to Ni based catalyst, the Rh ones exhibited higher carbon formation i.e. 10 mmol/gcat compared to 5.1 mmol/g cat at respective conditions. Higher selectivity to ethylene was observed over the Rh based catalyst resulting in higher carbon formation. At 900 °C, the Rh based catalyst exhibited higher activity as compared to the Ni based catalyst.

Simultaneous IMP was adopted by Dave and Pant [21] in SR of glycerol (SRG), in comparison to CP, POL, SG, and UH, IMP methods investigated by other authors. High activity was reported over 10 wt% Ni loading supported on 10 wt% zirconia promoted ceria. Addition of zirconia improved the crystallinity of the ceria which in turn improved the metallic dispersion there by affecting the activity of the catalyst. Further addition of zirconia resulted in a very small amount of methane being produced thus increasing the selectivity towards hydrogen.

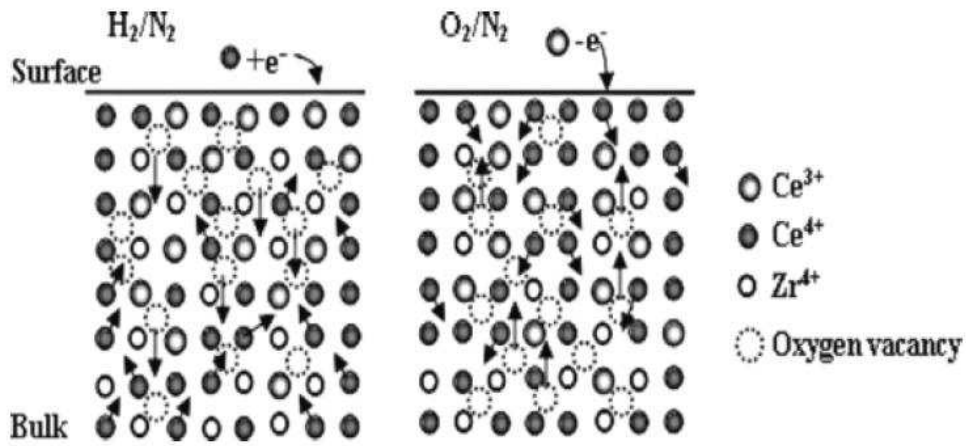


Fig. 4 A migration model of Ce^{4+} and oxygen vacancies during the reductive/oxidative treatment of ceria-zirconia mix oxide [40].

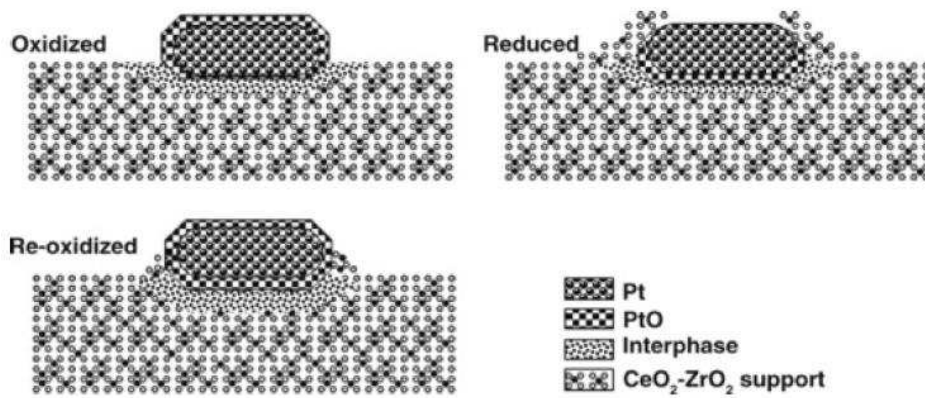


Fig. 5 A shell-core structure of Pt crystallites and the decoration/encapsulation by ceria-zirconia support during the reductive/oxidative treatments [40].

Table 5 Performance of Ce–Zr₂ supported metal catalysts in terms of hydrogen production obtained in SR of simple alkane and oxygenated hydrocarbons.

Author	Investigation	Conditions				Definition			Reported values		
		Catalyst	SC	Temp (C)	Yield Y (%)	Selectivity S (%)	Y (%)	S (%)	Conversion (%)	Molar comp (%)	
Vagia and Lemonidou [65]	SRA	0.5 wt% Rh–Ce _{0.15} Zr _{0.85} O ₂	3	750	23	–	90 ^a	–	100	–	
		5 wt% Ni–Ce _{0.15} Zr _{0.85} O ₂	–	–	–	–	85	–	100	–	
Zheng et al. [66]	SRA	12% Ni/7.5 wt% CeO ₂ -ZrO ₂	3	650	–	23	–	–85	100	–	
	SR of PFAD	5 wt% Ni–Ce _{0.75} Zr _{0.25} O ₂	3	900	–	–	–	70 ^b	100	–	
Roh et al. [62]	SRE	1 wt% Rh–Ce _{0.15} Zr _{0.85} O ₂	4	450	17	30	3.7	72	100	–	
Roh et al. [50]	SMR	12 wt% Ni–Ce _{0.2} Zr _{0.8} O ₂ -Al ₂ O ₃	1	800	–	–	85	–	83	–	
Roh et al. [47]	SMR	15 wt% Ni–Ce _{0.3} Zr _{0.7} O ₂	4	600	–	–	60.8 ^c	–	59.5 ^c	–	
Roh et al. [60]	SRE	2 wt% Rh–Ce _{0.2} Zr _{0.8} O ₂	4	450	–	–	4.08	–	40	–	
Laosripojana et al. [55]	SR of PFAD	5 wt% Rh–Ce _{0.75} Zr _{0.25} O ₂	3	800	19	–	56.7	–	–100 ^b	–	
Bliswas and Kunzru [19]	SRE	30 wt% Ni–Ce _{0.7} Zr _{0.3} O ₂	4	650	17	–	5.7	–	96.7	73.92	
Kusakabe et al. [45]	SMR	3 wt% Rh–Ce _{0.15} Zr _{0.85} O ₂	3	800	–	–	–	–	96.6	–	
		3 wt% Pt–Ce _{0.15} Zr _{0.85} O ₂	–	–	–	–	–	–	84.9	–	
		3 wt% Ru–Ce _{0.15} Zr _{0.85} O ₂	–	–	–	–	–	–	–	77.3	–
		10 wt% Ni–Ce _{0.15} Zr _{0.85} O ₂	–	–	–	–	–	–	–	66.6	–
Roh et al. [46]	SMR	10 wt% Ni–Ce _{0.2} Zr _{0.8} O ₂	3	750	22	–	115	–	–97 ^d	62 ^d	
Pojanavaraphan et al. [20]	SMRe	3 wt% Au–Ce _{0.75} Zr _{0.25} O ₂	2	400	–	–	–	–	>95	60	
Dave and Pant [21]	SRG	15 wt% CeO ₂ /10 wt% ZrO ₂	15.33 ^a	700	18	26	3.9	62.53	90.3 ^f	–	
Dong et al. [49]	SMR	30 wt% Ni–Ce _{0.2} Zr _{0.8} O ₂	3	750	–	–	–	>75	60.9	–	
Abreu et al. [51]	SMR	5 wt% Ni–Ce _{0.3} Zr _{0.7} O ₂ -Al ₂ O ₃	2.1	750	–	–	–	–	60	3.5 ^g	
		5 wt% Ni–Ce _{0.2} Zr _{0.8} O ₂ -Al ₂ O ₃	–	–	–	–	–	–	>70	2.4 ^h	
Laosripojana et al. [24]	SMR	5 wt% Ni–Ce _{0.75} Zr _{0.25} O ₂ (LSA) [†]	3	900	–	–	–	–	–50	–	
		5 wt% Ni–Ce _{0.75} Zr _{0.25} O ₂ (HSA)	–	–	–	–	–	–	>70	–	
Lin et al. [58]	SRE	10 wt% Co–Ce _{0.75} Zr _{0.25} O ₂	6.5	450	21	–	80	–	75	–	
Yan et al. [54]	SRA	12% Ni/7.5 wt% CeO ₂ -ZrO ₂	4.9	800	23	–	69.7	–	>55	–	

In table 5:

- a** In durability test at 650 °C activity decreased slightly in first 4 h, but remained fairly constant for next 11 h.
- b** The values were reported over a period of 50 h.
- c** The values were reported over 5 h of evaluations.
- d** The values were recorded over 200 min.
- e** Calculated based on 10 wt% glycerol solution.
- f** Conversion of glycerol into gaseous products.
- g** Highest molar composition was observed in first 50 min of evaluation decreasing slightly after that and remaining fairly constant for 350 min.
- h** Molar composition increased in first 50 min of the evaluation, remaining constant up till 250 min and decreasing further on up till the end of evaluation.
- i** LSA and HSA represent low and high surface area.
- j** The values were measured at 0.005 mol/h flow rate.

2.2 Autothermal reforming

Like SR, Ce–ZrO₂ supported catalysts have been investigated in ATR of hydrocarbons like methane, ethanol, glycerol, and bio-oils [68–70]. The following section describes the investigations of ceria–zirconia supported catalyst in ATR of simple alkane and oxygenated hydrocarbons.

2.2.1 Autothermal reforming of methane (ATRM)

The effect of catalyst preparation method over 0.1 wt% Rh/Ce_{0.5}Zr_{0.5}O₂ was investigated in ATRM by Cao et al. [71] using S/C of 2 and molar oxygen gas to carbon ratio (O₂/C) of 1.5 at 850 °C. The authors prepared catalysts using various methods like reverse micro-emulsion ('RME'), CP, urea combustion ('UC'), and SG. The findings suggested that reducibility and OSC of Ce_{0.5}Zr_{0.5}O₂ solid solution was significantly affected by the crystal structure. The best activity was reported for the catalyst prepared with ME, among the methods examined. The superior performance of the catalyst was attributed to a single cubic phase as opposed to tetragonal and mixed phases observed from the other methods. In contrast, Ruiz et al. [72] reported decreasing activity in ATRM over 1.5 wt% Pt supported on Ce_{0.5}Zr_{0.5}O₂ obtained using the AHCP method. The catalysts were tested using S/C of 0.2 and O₂/C of 0.5 at 800 °C. Deactivation occurred due to low Pt dispersion, resulting in low metal-support interfacial area. The lower OSC value along with larger Pt particle size reduced the carbon removal effectiveness of the catalyst, resulting in higher carbon deposition. Cubic phased Ce_{0.75}Zr_{0.25}O₂ showed the best performance among the formulations examined as a result of higher OSC, which helped in continuous removal of carbonaceous deposits from the active sites at the metal-support interfacial perimeter. Addition of small amount of carbon dioxide was useful in increasing methane conversion over Ce_{0.75}Zr_{0.25}O₂ based catalyst, but also affected catalyst stability after 24 h of evaluation.

Roh et al. [46] reported high activity in SMR of Ni/Ce_{0.2}Zr_{0.8}O₂ prepared by the SG method. The same catalyst exhibited higher activity under ATR conditions in comparison to SR. ATRM was performed using S/C of 3 over 15 wt% Ni supported on Ce_{0.2}Zr_{0.8}O₂ prepared using the MS method. Dong et al. [49] and Roh et al. [68] found that mobile oxygen species formed in the catalyst via a redox cycle enhanced decoking activity. Formations of composite layers of material were thought to be the reason for high activity. The composite was made of three different layers with top layer consisting of free Ni species followed by second layer of strongly interacted Ni and Ce ZrO₂ forming Ce Zr Ox, finally the last layer of Ce ZrO₂ support. Fig. 6 shows a schematic of the Ce–ZrO₂ catalyst structure

reported by Roh et al. [68]. The participation of the lattice oxygen was supplemented by the presence of O₂ molecules.

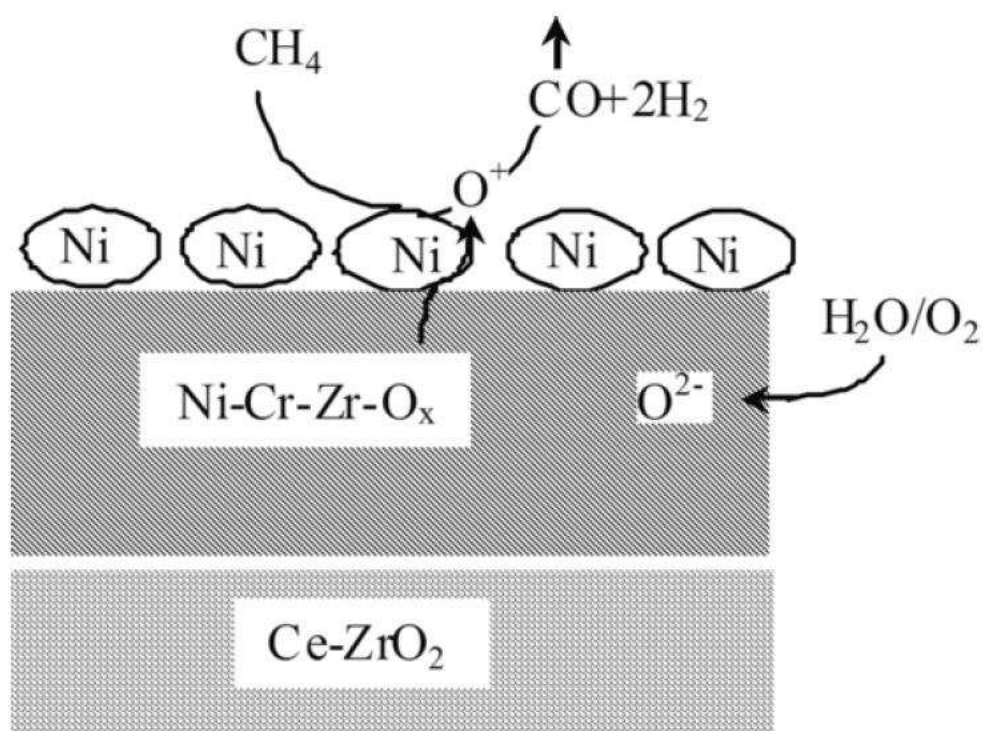


Fig. 6 Schematic of synthesis gas production over Ni/Ce-ZrO₂ catalyst [68].

Like Laosiripojana et al. [24], Lisboa et al. [73] reported high activity in ATRM over 10 wt% Ni supported on cubic phased Ce_{0.75}Zr_{0.25}O₂ support obtained using the CP method by means of AM and AH as co-precipitating agents. The process performance was examined at 800 °C using S/C of 2.5 and O₂/C of 0.5. The activity of the catalyst was attributed to a combination of metallic surface area and OSC of the support. Promotion effects of Ag, Fe, Pt and Pd in 10 wt% Ni supported on Ce_{0.5}Zr_{0.5}O₂ prepared using the CP method, for utilization in ATRM was investigated by Dantas et al. [74]. The performance of the catalyst was studied over harsher conditions i.e 800°C with S/C of 0.5 and O₂/C of 0.25. Addition of 1 wt% Ag was the best promoter. The catalyst reducibility along with the redox capacity of Ag containing catalyst was higher as compared to the bare Ni/Ce_{0.5}Zr_{0.5}O₂ catalyst. Lower loading of 0.1 wt% exhibited lower activity in comparison to the 1 Ag wt% promoted catalyst. Two different methods of IMP were examined, with co-IMP exhibiting higher activity in comparison to sequential IMP.

Addition of Al₂O₃ to tetragonal Ce_{0.8}Zr_{0.2}O₂ was shown by Roh et al. [50] to have a positive effect on performance of Ni supported catalyst in SMR. Escritori et al. [75] examined ATRM over Ni supported Ce_{0.5}Zr_{0.5}O₂ prepared using the AHCP method, followed by co-IMP of γ-Al₂O₃ to provide 12 wt%/Ce_{0.5}Zr_{0.5}O₂ modified Al₂O₃. Finally, a 10 wt% Ni was prepared by incipient wetness IMP of the modified support. The addition of Al₂O₃ favoured the formation of smaller Ni particles and better dispersion. The mix oxide based catalyst exhibited better reducibility compared to Ni/Al₂O₃. The presence of Ce-ZrO₂ helped to avoid carbon deposits on the catalyst by providing an additional path for the adsorption and dissociation of oxygen and steam, forming O₂⁻ and OH⁻ on the support surface. These groups removed the carbon deposits by reacting with them after they transferred to the metal-support interface. The presence of Zr in 10 wt%/Ni-

Zr₁₀Ce₂₀Al₇₀O₂ was reported to prevent the formation of the catalytically inactive phase NiAl₂O₄ and facilitate the dispersion of Ni, enhancing the activity of the catalyst [76].

2.2.2 Autothermal reforming of oxygenated compounds

De Lima et al. [77] reported high activity over 1.5 wt% Pt/Ce_{0.75}Zr_{0.25}O₂ under ATR conditions in comparison to SR in hydrogen production from ethanol. ATR of ethanol ('ATRE') was performed using S/C of 1 and O₂/C of 0.25 at 500 °C. In ATR conditions, decomposition of ethanol was inhibited or carbon monoxide oxidation was promoted. Further oxidative dehydrogenation of ethanol to form acetaldehyde was reported. In addition the oxidation of ethoxy species to acetate, followed by carbon dioxide formation as a result of decomposition via carbonates species, may use the oxygen from the support, as the vacancies were continuously replenished by oxygen from the feed. The presence of carbonate species on the catalyst surface were reported to be the reason for catalyst deactivation under SR conditions.

Youn et al. [69] examined the effect of Ce/Zr in ATRE using S/C of 1.5 and O₂/C of 0.25 at 500 °C. The support was prepared using the templating SG method followed by impregnation to get a Ni supported catalyst. A 20 wt% Ni supported on Ce_{0.7}Zr_{0.3}O₂ exhibited the best performance as a result of enhanced OSC of the support and the dispersion of Ni. The increase in Ce content beyond 0.7 resulted in lower activities due to excess oxygen provided by bulk ceria on the catalyst surface. Biswas and Kunzru [70] reported stable performance over 30 wt% Ni supported on Ce_{0.74}Zr_{0.26}O₂ catalyst in ATRE using S/C of 4 and O₂/C of 0.5 in the temperature range of 400 to 650 °C. Addition of oxygen up to a certain value was reported to have a positive effect on the activity of the catalyst. No change in Ni particle size was found after the catalytic evaluation reporting insignificant sintering of Ni particles. Performance of CeO₂-ZrO₂ in ATR of biobutanol was examined by Cai et al. [78]. The authors evaluated the use of 6.5 and 0.4 wt% Co-Ir supported on 18 wt% ceria containing CeO₂-ZrO₂ oxide in ATR of simulated bio-butanol mixture using S/C of 3 and O₂/mixture of 1.5 at 500 °C. The reducibility and OSC of the material affected the performance of the catalyst in descending order, following Co-Ir/18wt%CeO₂-ZrO₂ > Co-Ir/ZnO > Co-Ir/TiO₂.

Performance of Ce_{0.5}Zr_{0.5}O₂-Al₂O₃ in ATRE was reported by Srisiriwat et al. [79] using S/C of 1.5 and O₂/C of 0.13 at 700 °C. The addition of the mix oxide improved the dispersion of active Ni by inhibiting the interaction between Ni and Al₂O₃ support and promoting interaction between the support and the mix oxide. This addition of CeO₂ and/or ZrO₂ to Ni/Al₂O₃ enhanced the dissociation of intermediates from the oxygen fed into the system. This, further promoting the oxidation of hydrocarbons and carbon monoxide, produced from SRE to yield hydrogen and carbon dioxide. The oxygen intermediates effectively affected the (OSC) of the promoters, especially CeO₂ ZrO₂, by replenishing the oxygen vacancies in the ceria containing support, and in turn helping to reduce carbon formation. Kamonsuangkasem et al. [80] examined the use of 15 wt% Ni impregnated on 8%CeO₂-ZrO₂ modified Al₂O₃ in ATR of yellow glycerol. The best performance of the catalyst was reported over steam/glycerol and oxygen/glycerol molar ratios of 9 and 0.5 at 650 °C, respectively. The catalyst exhibited high oxidizing and reforming reaction activity.

In case of complex oxygenated hydrocarbons like ('PFAD'), Ni supported on the Ce_{0.75}Zr_{0.25}O₂, SACP method using ammonia ('AM') as a co-precipitation agent, exhibited higher activity under ATR conditions in comparison to SR of PFAD. Shotipruk et al. [56] examined effect of O₂/C in ATR of PFAD with fixed

S/C of 3 at 900 °C over 5 wt% Ni/Ce_{0.75}Zr_{0.25}O₂. Increase in O₂/C from 0 to 0.8 had a positive effect on hydrogen production, with higher ratios exhibiting no effect. The addition of oxygen was also shown to result in lower carbon formation formed from complex hydrocarbon fuels. Comparatively under same conditions Laosiripojana et al. [55] reported that with same metal loading, increase in O₂/C increased hydrogen production in ATR of PFAD up to a O₂/C value of 0.6 over Rh supported on Ce_{0.75}Zr_{0.25}O₂ prepared by the same method. Higher O₂/C had a negative effect on hydrogen production in comparison to no effect in case of a Ni based catalyst.

Table 6 below...

Table 6 Performance of Ce-ZrO₂ supported catalysts in terms of hydrogen production obtained in ATR of simple alkane and oxygenated hydrocarbons.

Author	Investigation	Catalyst	Conditions			Definition			Reported values		
			SC	O ₂ /C	Temp (C)	Yield Y (%)	Selectivity S (%)	Y (%)	S (%)	Conversion (%)	Molar comp (%)
Laosiripojana et al. [55]	ATR of PFAD	5 wt% Rh-Ce _{0.11} Zr _{0.2} O ₂	3	0.6	900	18			100 ^a	100 ^a	-
Sholjpruk et al. [56]	ATR of PFAD	5 wt% Ni-Ce _{0.07} Zr _{0.25} O ₂	3	0.8	900	-			80 ^b	100 ^b	-
Srisriwat et al. [79]	ATRE	15 wt% Ni-Ce _{0.12} Zr _{0.3} O ₂ -Al ₂ O ₃	1.5	0.13	700		32		-63.5 ^c	100 ^c	-
Roh et al. [68]	ATRM	15 wt% Ni-Ce _{0.2} Zr _{0.4} O ₂	1	0.5	750					99	-
Dong et al. [49]	ATRM	30 wt% Ni-Ce _{0.12} Zr _{0.25} O ₂	1	0.5	750					95	-
De Lima et al. [77]	ATRE	1.5 wt% Pt/Ce _{0.75} Zr _{0.25} O ₂	1	0.25	500	-	-			90 ^d	55
Cai et al. [78]	ATR of biobutanol	6.5 wt% Co-0.4 wt% Ir/18 wt%-CeO ₂ -ZrO ₂	3	1.5 ^a	500	-	-			86	68.5
Ruiz et al. [72]	ATRM	1.5 wt% Pt-Ce _{0.17} Zr _{0.25} O ₂	0.2	0.5	800	-	-			-70 ^e	-
Youn et al. [69]	ATRE	20 wt% Ni-Ce _{0.7} Zr _{0.3} O ₂	1.5	0.25	500		33		59	60 ^f	-
Cao et al. [71]	ATRM	30 wt% Ni-Ce _{0.12} Zr _{0.25} O ₂	2	0.45	850	-	26		52.96	57.62 ^f	-
Dantas et al. [74]	ATRM	1 wt% Ag-10 wt% Ni-Ce _{0.15} Zr _{0.15} -Al ₂ O ₃	0.5	0.25	800	-	-		80	55 ^g	-
Escribani et al. [75]	ATRM	10 wt% Ni-Ce _{0.12} Zr _{0.5}	0.5	0.25	800	-	-		-	>40 ^h	~48 ^h

table 6 continues..

2.3 Catalytic partial oxidation

CPO over various noble and base metals supported on Ce–ZrO₂ has been examined by Salazar-Villalpando et al. [81], Salazar-Villalpando and Miller [82] Salazar-Villalpando and Reyes [83], Larimi and Alavi [84], Silva et al. [85], and Silva et al. [86]. Investigations of ceria–zirconia supported catalyst in PO of hydrocarbon and oxygenated hydrocarbon are reviewed in the following sections.

2.3.1 Catalytic partial oxidation of methane (CPOM)

Salazar-Villalpando's group [81–83,87] examined the CPOM at 700 °C using O₂/C of 5 over 1 wt% Rh, Pt and Ni supported on cubic Ce_{0.56}Zr_{0.44}O₂, prepared by the CP method followed by hydrothermal crystallization. The Rh supported catalyst exhibited the highest activity as a result of the reducibility of material. Redox cycling of the material was shown to affect hydrogen generation by improving catalytic performance. Lattice oxygen was found to selectively oxidize methane to form carbon monoxide [87] through isotopic studies. Further, the presence of Rh accelerated the oxygen exchange with the support with maximum value observed at 250 °C. This was a result of oxygen spill over from the metal to the support. In comparison to the Rh supported catalyst, higher activity was found for Pt supported ones [82]. They reported that Ce anchored metallic Pt and helped in maintaining surface area along with prevention of migration and coalescence of Pt crystallites. PtO₂ present in the catalyst was reduced by methane, decreasing the amount of PtO₂ in the catalyst. Thus Pt reducibility was maintained thereby suppressing Pt sintering via formation of mobile and volatile PtO₂. It was suggested that the high stability of Pt in Ce–containing supports under oxidizing conditions at high temperature was due to the formation of a Pt O Ce bond. This result was in contrast to that reported by de Lima et al. [63] in SRE using 1.5 wt% Pt/Ce_{0.75}Zr_{0.25}O₂ catalyst.

Passos et al. [88] reported a different reason for higher stability of Pt supported catalysts in CPOM at 800 °C with O₂/C of 0.5. They examined the performance of 1.5 wt% Pt over supports i.e. Ce_{0.75}Zr_{0.25}O₂, Ce_{0.5}Zr_{0.5}O₂ and Ce_{0.25}Zr_{0.75}O₂ prepared by the CP method using ammonium hydroxide (AH) as a co-precipitating agent. Support reducibility and metal dispersion were the two important reasons for high stability of the Pt supported catalyst. The performance of the catalyst was also attributed to proper balance between OSC of the support and metal dispersion over the catalyst. The higher OSC of the material helped in removing the carbon deposits from the metal-support interface. Among the support formulations Ce_{0.5}Zr_{0.5}O₂ exhibited lower deactivation in comparison to Ce_{0.75}Zr_{0.25}O₂ and Ce_{0.25}Zr_{0.75}O₂. A lower metal dispersion over the support decreased the metal-support interfacial area and hence the effectiveness of the carbon removal mechanism. Similar explanations regarding reducibility and OSC for high activity over 1.5 wt% Pt/Ce_{0.75}Zr_{0.25}O₂ were reported by Mattos et al. [89,90] in CPOM at 800 °C using O₂/C of 2. The supports were prepared by using the AHCP method. Combustion of methane was reported to be the first step during the process leading to the formation of carbon dioxide and steam, production of synthesis gas followed via DR and SR of the unreacted methane. Similarly 3–5 wt% Pd/Ce_{0.7}Zr_{0.3}O₂ exhibited high activity in CPOM between 700 and 900 °C, Fangli et al. [91]. The conversion over Pd catalyst was slightly lower compared to those over Pt and Rh ones. The activity of the catalyst was reported to be caused by higher dispersion of Pd and OSC capacity of the support. Unlike other noble metals i.e. Pt, Rh, and Pd, the supported Ru catalyst exhibited lower activity [92].

Performance of Pt supported on $\text{Ce}_{0.75}\text{Zr}_{0.25}\text{O}_2\text{-Al}_2\text{O}_3$ catalyst was affected by Pt loading in CPOM at 800 °C with O_2/C of 0.5, Silva et al. [85]. The doped support and active metal was prepared by the wet IMP method. The catalysts with higher dispersion (lower loading 0.5 wt%) promoted methane decomposition. Since the OSC of the support was not affected by Pt dispersion, the increased methane decomposition led to imbalance in the OSC and thus carbon deposition, leading to deactivation. In contrast, Silva et al. [93,94] found that 1.5 wt% Pt/ $\text{Ce}_{0.75}\text{Zr}_{0.25}\text{O}_2\text{-Al}_2\text{O}_3$ exhibited lower activity under the same conditions. The lower activity of the catalyst was attributed to lower surface coverage and OSC. Further, Zr incorporation in the ceria lattice was not achieved using the IMP method, affecting the activity of the catalyst. Similarly the activity of the catalyst was lower in comparison to Pt/ $\text{CeO}_2/\text{Al}_2\text{O}_3$.

The effect of support preparation methods on the performance of the catalyst was further examined by Silva et al. [86]. The supports were prepared with the PP and IMP methods, the latter providing higher surface coverage and resulting in higher stability and selectivity to hydrogen and carbon monoxide [86]. Under same conditions, addition of 1 wt% Ce to Al_2O_3 , was shown by Silva et al. [95] to improve the performance of a Pt/ $\text{Ce}_{0.75}\text{Zr}_{0.25}\text{O}_2\text{-Al}_2\text{O}_3$ catalyst, by improving Pt dispersion, OSC, and coverage of Al_2O_3 by oxides. The addition of Ce helped in the formation of a more homogeneous solid solution affecting the performance as a result of higher OSC. The effect of Ce–Zr content on the performance of 1.5 wt% Pt/ $\text{Ce}_{0.5}\text{Zr}_{0.5}\text{O}_2\text{-Al}_2\text{O}_3$ in CPOM at 800 °C with O_2/C was examined by Silva et al. [96]. Catalysts containing 10 to 20 wt% mix oxides were reported to form a solid solution, in comparison to 30 wt% which showed ceria rich and a zirconia rich phases, whereas 40 wt% exhibited a ceria rich phase and an isolated zirconia phase. Catalysts with 10 and 20 wt% Ce– ZrO_2 had high activity in comparison to the others. The effect of support calcination temperature on the activity of 1.5 wt% Pt/ $\text{Ce}_{0.5}\text{Zr}_{0.5}\text{O}_2\text{-Al}_2\text{O}_3$ in CPOM was examined by Mortola et al. [97]. The supports were calcined at 800, 900, and 1000 °C with activity evaluation performed at 800 °C with O_2/C of 0.5. Supports calcined at 800 and 900 °C showed slight decrease in activity in comparison to the significant decrease exhibited by the support calcined at 1000 °C. At all the calcination temperatures the supports showed formation of heterogeneous instead of homogenous solid solution. Surface area, degree of Al_2O_3 surface coverage by the ceria-based oxide, metallic dispersion, along with OSC decreased during the aging process at 800 and 900 °C. In addition to these effects, at 1000 °C ceria particle size increased as a result of sintering, deteriorating the stability of the catalyst. Although the supports aged at 800 and 900 °C affected the above properties of the catalyst, the reduction in these properties were not as significant as compared to those of the catalyst aged at 1000 °C, hence these catalyst exhibited higher activity and stability and selectivity to hydrogen and carbon monoxide.

Increase in Rh dispersion along with activity for WGS and oxygen mobility due to the presence of ceria, was reported as the cause of higher activity of Rh/ $\text{Ce}_{0.5}\text{Zr}_{0.5}\text{O}_2\text{-Al}_2\text{O}_3$. Boullousa-Eiras et al. [98] examined CPOM over 0.1 to 0.3 wt% Rh supported on $\text{Ce}_{0.5}\text{Zr}_{0.5}\text{O}_2\text{-Al}_2\text{O}_3$ using O_2/C 0.5 from 600 to 1250 °C. Further the high activity of the catalyst was also reported, due to the presence of stabilised Al_2O_3 along with the inhibition of α and CeAlO_3 phases, which are known to be responsible for worse stability of $\text{CeO}_2/\text{Al}_2\text{O}_3$ supported catalysts. Two different methods of preparation of the catalyst i.e. spray drying and slow evaporation were examined. Spray drying support had the highest thermostability in terms of sintering and phase transformation of the composites [99]. In addition to noble metals like Pt, and Rh, Ni supported on $\text{Ce}_{0.7}\text{Zr}_{0.3}\text{O}_2/\text{Al}_2\text{O}_3$ was evaluated in CPOM by Qingwei et al. [100]. The performance of catalyst prepared by two different methods was examined in CPOM using O_2/C of 0.5

between 600 and 900 °C. Catalyst formulation prepared by physical mixing of Al₂O₃ and Ce–ZrO₂ displayed the poorest performance, while the catalyst prepared by AMCP of Ce(NO₃)₂ and Zr(NO₃)₂ (mix solution) along with Al(NO₃)₃, presented the best performance. But the carbon deposition on the catalyst prepared by the CP method was higher in comparison to the physically mixed formulation.

Like Rh/Ce_{0.56}Zr_{0.44}O₂, the Ni supported catalyst was reported to require redox pre-treatments to reach higher catalytic activity [83]. The increase in activity in case of Ni was seen as a result of metallic re-dispersion and changes on the metal support interface. Dong et al. [101] and Roh et al. [102] reported divergent results over 15 wt% Ni supported Zr-rich supports (Ce_{0.2}Zr_{0.8}O₂) prepared by the molten salt sol gel ('MSSG') method using O₂/C of 0.5 between 600 and 800 °C. Dong et al. [101] performed CPOM using a pulse mechanism. Methane adsorbed on the Ni surface and dissociated to form hydrogen and carbon. The carbon then reacted with oxygen which was activated on Ni to form carbon monoxide. Similarly some carbon traveled to the interface of Ni Ce ZrO₂ and Ni, reducing the support near the metallic Ni particle to produce carbon monoxide. Some of the carbon adsorbed on the metallic Ni was removed by the use of the lattice oxygen in the Ce ZrO₂ support. The oxygen species was replenished by the gaseous oxygen. The dissociation of methane was enhanced as a result of the Ce_{0.2}Zr_{0.8}O₂ support and improved carbon storage. Further, the mobility of oxygen promoted carbon removal from the catalyst surface. Larimi and Alavi [84] examined the performance of CPOM over 5 wt% Ni supported on Ce–ZrO₂ prepared by the sodium hydroxide co-precipitation ('SHCP') method at 700 °C with O₂/C of 0.5. Conversion of methane was reported to increase with Zr content, similarly to that reported by Dong et al. [49] and Roh et al. [102]. The increase in Zr content increased the catalyst surface area and Ni dispersion, thus increasing the activity of the catalyst. A catalyst formulation of Ce_{0.25}Zr_{0.75}O₂ exhibited the best performance with least carbon deposition among the formulations examined. Under similar conditions, the results were very close to those reported by Wang and Xu [103] and Pengpanich et al. [104] over 10 and 15 wt% Ni supported on Ce_{0.25}Zr_{0.75}O₂ obtained using AMCP and UH methods respectively. Larrondo et al. [105] examined the performance of Ni supported on Ce_{0.9}Zr_{0.1}O₂ in CPOM using O₂/C 0.5 from 400 to 800 °C. They found the bare Ce_{0.9}Zr_{0.1}O₂ support could be utilized as methane oxidation catalyst. Also, Ni/Ce_{0.9}Zr_{0.1}O₂ acted as an oxidation catalyst up to 650 °C. Above 650 °C, the catalyst behaved as a CPO catalyst producing reformat with a H₂/CO of 2. The mobility of oxygen in the material resulted in inhibition of carbon deposits. Higher Ni loading exhibited higher conversion. Villalpando et al. [83] reported that the Ni supported catalyst exhibited higher activity as a result of higher reducibility and surface area. The higher reducibility of the catalyst resulted in increased availability of surface lattice oxygen, which participated in the formation of carbon monoxide and hydrogen. Similarly the catalyst was reported to exhibit high ionic conductivity affecting the amount of carbon formed during the CPOM reaction at lower O₂/C of 0.6. High oxygen mobility was also reported to accelerate surface carbon oxidation reactions, inhibiting carbon growth.

2.3.2 Catalytic partial oxidation of oxygenated hydrocarbons

In comparison to CPOM there are very few evaluations of hydrogen production over Ce–ZrO₂ using ('CPOE') and other oxygenated hydrocarbons. CPOE at 300 °C and O₂/C of 1 over 1.5 wt% Pt supported on Ce_{0.5}Zr_{0.5}O₂ prepared using the AHCP method was examined by Mattos et al. [106]. The presence of ceria in the catalyst was responsible for the presence of methane and carbon dioxide via the

formation of acetate as a result of the OSC of the material. In contrast, the ZrO₂ based catalyst was responsible for the formation of acetaldehyde via dehydrogenation of ethoxy species. The catalyst showed higher selectivity towards ethoxy species in comparison to the ceria based catalyst. A 1.5 wt% Pt/Ce_{0.75}Zr_{0.25}O₂ prepared by the same method did not produce the desired hydrogen in CPOE at 500 °C with O₂/C of 0.25 [77]. Instead, the catalyst had high selectivity towards acetaldehyde and carbon dioxide during CPOE. In a different investigation Wang et al. [107] reported that 20 wt% Ni supported on Ce_{0.8}Zr_{0.2}O₂ prepared by glycine nitrate process demonstrated high activity in CPOE at O₂/C of 1 in the temperatures range of 450 to 700 °C. Quite high selectivity to hydrogen was measured at 500 °C. The catalyst also displayed high resistance to carbon formation in SMR similar to the above applications. Ce_{0.75}Zr_{0.25}O₂ was also found to have high activity in CPO of complex oxygenated hydrocarbons like palm fatty acids ('PFA'). Laosiripojana et al. [108] examined the performance of PO of palm fatty acid distillate (PFAD) at 850 °C with O₂/C of 1 using a 5 wt% Ni supported on Ce_{0.75}Zr_{0.25}O₂ prepared by the SACP method using urea as precipitating agent. The high activity of the catalyst prepared by the SACP method in comparison to the one prepared by the conventional CP method, was attributed to nano sized Ce–ZrO₂ support and higher OSC and lattice oxygen mobility. The authors also reported that higher oxygen or temperature inhibited the formation of the higher hydrocarbons like ethylene, ethane, and propylene.

Table 7 below (2 pages)

Table 7 summarizes the performance evaluations of various metal supported Ce-ZrO₂ supported metal catalysts in CPO of simple alkanes and oxygenated hydrocarbons.

Author	Investigation	Conditions			Definition			Reported values		
		Catalyst	O ₂ /C	Temp (C)	Yield Y (%)	Selectivity S (%)	Y (%)	S (%)	Conversion (%)	Molar comp (%)
Laacirpojana et al. [108]	CPO of PFAD	5 wt% Ni-Ce _{0.8} Zr _{0.2} O ₂	1	900	20		70		100	-
Larrondo et al. [105]	CPOM	50 wt% Ni-Ce _{0.3} Zr _{0.7} O ₂	0.5	650		28		-118	100	-
		9 wt% Ni-Ce _{0.9} Zr _{0.1} O ₂						-108	90	
Pengpanidh et al. [104]	CPOM	15 wt% Ni-Ce _{0.25} Zr _{0.75} O ₂	0.5	750		29		91	98	-
Larimi and Alavi [94]	CPOM	5 wt% Ni-Ce _{0.25} Zr _{0.75} O ₂	0.5	850				95	-98	-
Dong et al. [49]	CPOM	15 wt% Ni-Ce _{0.2} Zr _{0.8} O ₂	0.5	800				99.6	98	
Farghi et al. [91]	CPOM	3.0 wt% Pt-Ce _{0.1} Zr _{0.9} O ₂	0.5	800					92.8 ^a	-
		5.0 wt% Pt-Ce _{0.1} Zr _{0.9} O ₂							92.6 ^b	
		1.0 wt% Pt-Ce _{0.1} Zr _{0.9} O ₂							72.6 ^b	
F. Silva et al. [95]	CPOM	1.5 wt% Pt/Ce _{0.2} Zr _{0.8} O ₂ /1 wt% Ce-Al ₂ O ₃	0.5	800					60 ^a	90 ^a
F. Silva et al. [85]		0.5 wt% Pt/Ce _{0.2} Zr _{0.8} O ₂ /Al ₂ O ₃							60 ^a	90 ^a
		1.0 wt% Pt/Ce _{0.2} Zr _{0.8} O ₂ /Al ₂ O ₃							60 ^a	90 ^a
		1.5 wt% Pt/Ce _{0.2} Zr _{0.8} O ₂ /Al ₂ O ₃							60 ^a	90 ^a
Xu and Wang [103]	CPOM	10 wt% Ni-Ce _{0.25} Zr _{0.75} O ₂	1.88	750					-	85
Salazar-Villalpando et al. [81]	CPOM	1 wt% Rh-Ce _{0.6} Zr _{0.4} O ₂							90 ^b	83 ^b
Roh et al. [102]	POM	1.5 wt% Pt-Ce _{0.2} Zr _{0.8} O ₂	1.87	750					98	>80
F. Silva et al. [96]	CPOM	1.5 wt% Pt/10% Ce _{0.2} Zr _{0.8} O ₂ /Al ₂ O ₃	0.5	800					95 ^c	-70 ^c

		1.5 wt% Pt/30% Ce _{0.33} Zr _{0.33} Al ₂ O ₃				95 ^e	-67 ^c	
		1.5 wt% Pt/40% Ce _{0.2} Zr _{0.3} O ₂ /Al ₂ O ₃				95 ^d	-67 ^d	
		1.5 wt% Pt/20% Ce _{0.33} Zr _{0.33} O ₂ /Al ₂ O ₃				95 ^d	-65 ^d	
Maitos et al. [89,90]	CPOM	1.5 wt% Pt-Ce _{0.33} Zr _{0.4} O ₂	0.5	800	-	-80 ^a	>80 ^a	-
Mortola et al. [97]	CPOM	1.5 wt% Pt/10%Ce-ZrO ₂ /Al ₂ O ₃	0.5	1000	-	100 ^o	60 ^o	-
		1.5 wt% Pt/10%Ce-ZrO ₂ /Al ₂ O ₃		900		-92 ^o	-58 ^o	
		1.5 wt% Pt/10%Ce-ZrO ₂ /Al ₂ O ₃		800		-92 ^o	-58 ^o	
Passos et al. [98]	CPOM	1.5 wt% Pt-Ce _{0.33} Zr _{0.4} O ₂	2	800	-	>80 ^b	-60 ^b	-
P Silva et al. [94]	CPOM	1.5 wt% Pt-Ce _{0.2} Zr _{0.5} O ₂ -Al ₂ O ₃	0.5	800	-	-85	-52	-
		1.5 wt% Pt-Ce _{0.22} Zr _{0.75} O ₂ -Al ₂ O ₃				-85	-52	
		1.5 wt% Pt-Ce _{0.15} Zr _{0.25} O ₂ -Al ₂ O ₃				90	50	
		1.5 wt% Pt-Ce _{0.17} Zr _{0.25} O ₂ -Al ₂ O ₃ imp ^l				90 ^l	50 ^l	
P Silva et al. [96]		1.5 wt% Pt-Ce _{0.17} Zr _{0.25} O ₂ -Al ₂ O ₃ -ppp				90 ^o	50 ^o	
Dong et al. [101]	CPOM	15 wt% Ni-Ce _{0.2} Zr _{0.4} O ₂	0.5	800			27.4 ^h	-
Salazar-Villalpando and Reyes. [83]	CPOM	1 wt% Ni-Ce _{0.33} Zr _{0.44} O ₂	0.4-0.8	700	-	-	-	-4-5
		1 wt% Ni-Ce _{0.33} Zr _{0.44} O ₂ -redox pre				.	.	-9

^a The activity was measured over period of 24 h.

^b The activity was measured for 1200 min.

^c The values were measured and were constant for the period examined.

^d The values decreased within the evaluation of 24 h.

^e The conversion and hydrogen selectivity for supports aged at 800 and 900 °C decreased slightly. While the samples aged at 1000 °C, decreased to 40 % by end of 24 h evaluation.

^f Catalyst prepared by the IMP method. The catalytic activity in terms of conversion and selectivity was stable for 24 h.

^g Catalyst prepared by the PP method. The conversion decreased to 20% within 24 h. While selectivity decreased to 40 % within 24 h.

^h The results obtained are for one second pulse.

2.4 Dry reforming

Carbon dioxide has been identified as the most significant greenhouse gas arising from anthropogenic activities. Conversion of carbon dioxide is presently being explored as one potential alternative to its geological sequestration. Production of useful value-added products (chemicals products, fuels ...) via syngas production and by dry reforming of methane ('DRM') has been investigated [109–113]. A major drawback of the process is formation of carbon over the catalyst surface. Ce–ZrO₂ supported catalysts have been known to impart high activity in DRM as a result of high OSC of the support which generates active centers at the interface between metal and support, helping in decoking ability of the catalyst. In addition the presence of ceria has been shown to improve dispersion of the metal on the support, improving the catalytic activity.

Pt supported on ceria–zirconia catalyst exhibited poor performance in DRM at 600 °C with CH₄/CO₂ of 1. Damyanova et al. [114] examined the performance of 1 wt% Pt impregnated on CeO₂ promoted ZrO₂ with CeO₂ content varying from 1 to 12 wt%, using CH₄/CO₂ ratio of 1 at 600 °C. Increase in ceria content from 1 to 12 wt% decreased CH₄ conversion, while increase in ceria content from 1 to 6 wt% increased CO₂ conversion and upon further increase in ceria content it decreased, finally yielding conversion values as low as 18% and 23% for CH₄ and CO₂ respectively. Similarly Chen et al. [115] found Rh supported on Ce_{0.752}Zr_{0.250}O₂ catalyst exhibited a performance similar to Pt/CeO₂–ZrO₂ at 600 °C with CH₄/CO₂ of 1. The catalyst supports were prepared by SACP method. Increase in temperature and Ru loading resulted in higher catalytic activity. Higher Ru content (3 wt%) increased the activity of the catalyst due to higher Ru surface area. Lower loading (0.5 wt%) resulted in a strong interaction between support and metal, leading to lower availability of Ru for the reaction, and hence lower activity. However the increase in Ru loading above 1.5 wt% affected the stability of the catalyst by decreasing the surface areas and pore volumes of the catalysts.

Formations of hydroxides were reported to occur during the reforming reaction responsible for carbon elimination. Unlike noble metals supported on Ce–ZrO₂, Ni based catalysts have exhibited higher catalytic activity. Potdar et al. [116] assessed the use of 15 wt% Ni supported Ce_{0.8}Zr_{0.2}O₂ catalyst in DRM prepared by a CP/digestion method. The authors compared the performance of a catalyst prepared using the CP method with an impregnated one at 800 °C using CH₄/CO₂ of 1. The catalyst prepared by the CP method exhibited the best performance. The high activity of the catalyst was due to higher surface area of the nanosized support along with the better dispersion of NiO particles, and the strong integration of support and metal.

Roh et al. [117,118] examined the performance of DRM at 800 °C and CH₄/CO₂ of 0.96 over Ni catalyst prepared using the potassium hydroxide co-precipitation ('PHCP') method. The effect of support composition on the performance of the catalyst was investigated, with Ce_{0.2}Zr_{0.8}O₂ and Ce_{0.5}Zr_{0.5}O₂ showing severe deactivation as a result of carbon formation. Like Potdar et al. [116] they reported that Ni–Ce_{0.8}Zr_{0.2}O₂ catalyst prepared by CP method, had the best performance among the compositions examined. The catalyst's performance was also better in comparison to the catalyst prepared by Ni impregnated on Ce_{0.8}Zr_{0.2}O₂ support. Both groups examined the effect of loading on the catalyst performance, with 15 wt% Ni/Ce_{0.8}Zr_{0.2}O₂ performing best among the catalysts prepared by both the methods. Higher loading resulted in carbon formation over the catalyst, attributed to lower Ni dispersion and higher Ni particle size. At similar conditions Jun et al. [119] also reported high activity over 15 wt% Ni/Ce_{0.8}Zr_{0.2}O₂ formulation as a result of the combined effect of the nano crystalline cubic Ce_{0.8}Zr_{0.2}O₂ support and the fine dispersion of the NiO_x crystallites, leading to intimate contact between metal and support. Like Roh et al. [120], they examined the performance of Ce_{0.2}–

Zr_{0.8}O₂/θ-Al₂O₃ in DRM at same conditions. Addition of Ce–ZrO₂ to Al₂O₃ inhibited the transformation of Ni/θ-Al₂O₃ into NiAl₂O₄, and led to the formation of active NiO_x thus imparting higher activity and stability to the catalyst. Under reforming conditions the catalyst was reported to be oxidized, which in turn reacted with deposited carbon, deoxidised by carbon dioxide dissociation. Increasing Ni loading from 3 to 6 wt% slightly affected the performance, but higher loading from 12 to 15 wt% had no effect.

Addition of Mg to Ce_{0.8}Zr_{0.2}O₂ had a positive effect on the performance of the catalyst in DRM. Jang et al. [121] examined the performance using 15 and 10 wt% Ni and MgO over the supports at 800 °C. Addition of Mg to Ni/Ce_{0.8}Zr_{0.2}O₂ reduced the degree of reduction of the catalyst, and resulted in the formation of a solid solution between Ni and MgO. The basicity of MgO resulted in higher resistance of nickel to sintering and created intimate contact between Ni and MgO, causing a higher catalytic activity.

Co supported on Ce_{0.8}Zr_{0.2}O₂ was also reported to exhibit high activity in DRM. Wang et al. [122] studied the use of 16 wt% Co supported on Ce_{0.8}Zr_{0.2}O₂ prepared by the PHCP method, in DRM at 750 °C using CH₄/CO₂ of 1. The charge effect of CoO_x species along with cubic Ce_{0.8}Zr_{0.2}O₂ improved the reducibility of the sample. Further cubic Ce_{0.8}Zr_{0.2}O₂ decreased the Co crystallite sizes and resulted in lower carbon deposition on the surface of the catalyst.

Kumar et al. [123] looked at the effect of catalyst preparation methods on the performance of 5 wt% Ni supported on ceria-zirconia catalyst in DRM at 700 °C with CH₄/CO₂ of 1. The catalyst supports were prepared using the SA aqueous AMCP method, and were compared with SG (alco-gel) prepared supports followed by Ni IMP. The SA supports exhibited better performance than the alco-gel prepared ones, due to higher surface area resulting in higher Ni dispersion on the support, along with better thermal stability. In comparison to the above authors [116,118,119], a 5 wt% Ni/Ce_{0.6}Zr_{0.4}O₂ exhibited the best performance among the various compositions of supports prepared. Higher reducibility of the support enabled the support to make use of OSC and participate in redox reactions enhancing the stability of the catalyst. Unlike the above authors Ni on support prepared by the AMCP method exhibited lower activity.

The effect of surfactant addition to supports prepared using the AMCP method, in DRM was investigated by Sukonket et al. [124]. Catalyst supports prepared using higher surfactant/metal molar ratio exhibited higher activity. Performance of the catalyst was studied at 800 °C over 5 wt% Ni/Ce_{0.6}Zr_{0.4}O₂ using CH₄/CO₂ ratio of 1. Higher amount of surfactant led to a better dispersion of Ni on the catalyst leading to a stable catalyst formulation. The amount of surfactant affected the OSC of the catalyst, increasing with the amount of surfactant. The catalyst support prepared by metal/surfactant ratio of 1.25 possessed the largest numbers of both surface-active Ni sites and oxygen vacancies resulting in higher activity. Similar results were reported by Chen et al. [125] over 2 wt% Ni–Ce_{0.75}Zr_{0.25}O₂ prepared using the 25% aqueous AMCP method, using CH₄/CO₂ of 1 in the temperature range of 700 to 900 °C. Methane conversion was shown to increase with rise in temperature. Addition of Ni to the solid solution in the co-precipitated catalyst resulted in better Ni dispersion and stronger interactions between Ni and the solid solution. Also the co-precipitated catalyst exhibited higher surface area and pore volume, resulting in the formation of catalyst with high activity along with higher resistance to coke formation and Ni sintering.

Matralis et al. [126] examined the DRM over 5 wt% Ni supports prepared by means of the AMCP method, with varying Ce/Zr ratio at 700 °C at CH₄/CO₂ of 1 without dilution. The authors reported that the Ce/Zr did not have a significant effect on the activity of the catalyst although surface areas and the surface of the metallic Ni varied considerably. Unlike Kumar et al. [123], Potdar et al. [116] and

Roh et al. [117], they reported that Zr rich supports had higher activity and higher resistance to carbon formation. Fig. 7 shows the mechanism of DRM over Ni based catalysts supported on mesoporous nanocrystalline ceria–zirconia solid solutions [127].

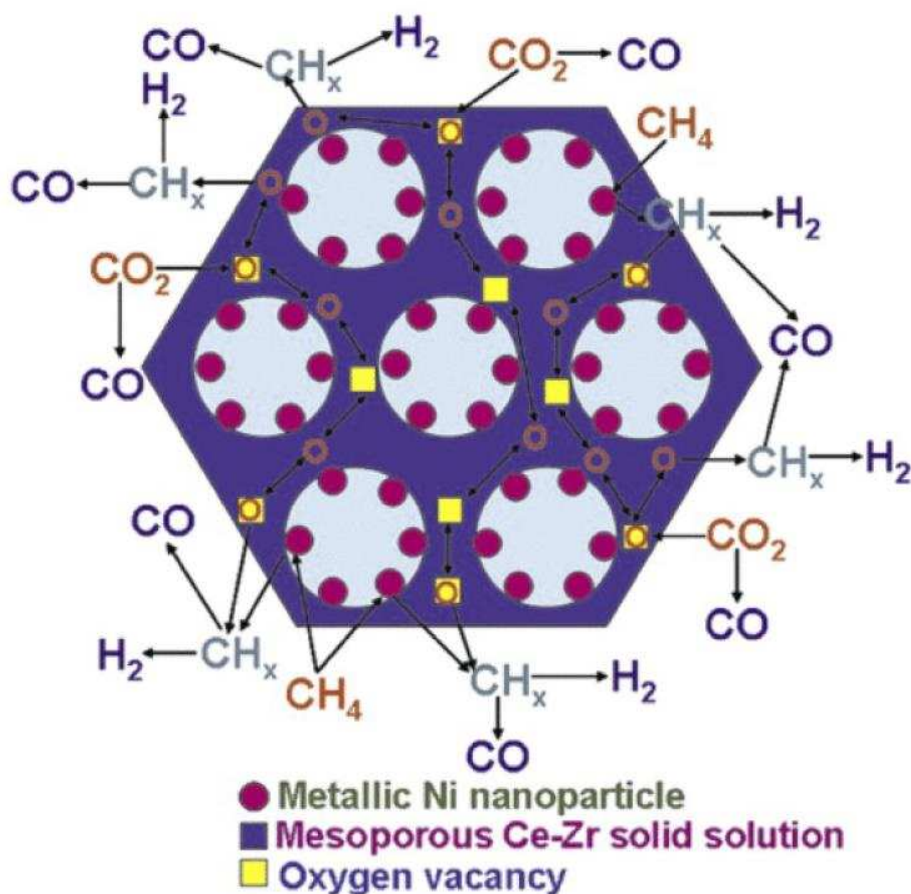


Fig. 7 Mechanism of the DRM over Ni based catalysts supported on mesoporous nanocrystalline ceria–zirconia solid solutions [127].

Most of the above authors utilized CP or SACP methods using various CP agents like PH and AM, but Črnivec et al. [128] compared the performance of Ce_{0.8}Zr_{0.2}O₂ prepared using AMCP and glycothermal assisted methods for DRM. The performance of the catalysts were investigated at 800 °C using an undiluted mixture of methane and carbon dioxide. Materials synthesized using the CP method resulted in the formation of larger size crystallites of segregated CeO₂ and ZrO₂ oxides exhibiting poor activity and lower carbon resistance. In the glycothermal method, ethylene glycol and propanoic acid were reported to act as surface directing agents regulating the nanostructural assembly of the supports, resulting into a homogeneous nanocrystalline solid. The PP deposition method, used for laying down Ni on the support, resulted in the formation of smaller Ni particles; in comparison to the Ni particles obtained by the simple deposition method. The smaller Ni particles caused superior resistance to surface carbon and also displayed certain selectivity for the RWGS reaction. Table 8 summarizes the performance evaluations of Ce–ZrO₂ supported metal catalysts in DR of simple alkanes and oxygenated hydrocarbons.

Table 8 Performance of Ce–ZrO₂ supported catalysts in terms of hydrogen production obtained in DR of simple alkane and oxygenated hydrocarbons.

Author	Investigation	Conditions			Definition			Reported values		
		Catalyst	CO ₂ /CH ₄	Temp (C)	Yield Y (%)	Selectivity S (%)	Y (%)	S (%)	Conversion (%)	Molar comp (%)
Jun et al. [119]	DRM	15 wt%Ni–Ce _{0.8} Zr _{0.2} O ₂	0.98	800	–	–	–	95	98 ^a	–
		15 wt%Ni–Ce _{0.2} Zr _{0.8} O ₂			–	–	–	–	90 ^b	–
		15 wt%Ni–Ce _{0.2} Zr _{0.8} O ₂			–	–	–	–	91 ^c	–
		5 wt%Ni–Ce _{0.2} Zr _{0.8} O ₂			–	–	–	–	80 ^d	–

table 8 continued

3 Conclusion

Hydrogen production using Ce–ZrO₂ supported catalysts during steam reforming, autothermal reforming, catalytic partial oxidation, and dry reforming of simple alkanes such as methane, and of oxygenated hydrocarbons like ethanol, glycerol, and acetic acid were reviewed. Among the processes examined steam reforming and autothermal reforming have demonstrated highest efficiencies and hydrogen yields. The performance of the Ce–ZrO₂ catalyst is greatly affected by the method of preparation, surface area, metal dispersion and reducibility of the catalyst. Methods of catalyst preparation were shown to affect the oxygen storage capacity of the Ce–ZrO₂ catalyst thus affecting its resistance to carbon deposition. Among the various evaluations, the co-precipitation method has been widely investigated in hydrogen production using all the process reviewed, in particular for the methane feedstock. Further addition of surfactant during the co-precipitation method helped to increase the surface area, and resistance to coke and to Ni sintering.

Only the steam and autothermal reforming processes have been investigated for hydrogen production from oxygenated hydrocarbons. Utilization of Ce–ZrO₂ support for catalytic partial oxidation and dry reforming of oxygenated hydrocarbons has not been investigated extensively. A single hydrogen production evaluation via partial oxidation of PFAD over Ni/Ce–ZrO₂ was reported. In the temperature range examined (450 to 900 °C), Ce rich (Ce \geq 0.5) catalysts were reported to be effective in steam reforming, autothermal reforming, and catalytic partial oxidation of oxygenated hydrocarbons. In the case of methane, different support compositions offered effective results at different temperatures. Noble metals and Ni supported on Ce rich (Ce \geq 0.5) supports were shown to be effective for steam methane reforming throughout the temperature range, while Ni supported on Zr rich (Ce \geq 0.2) were reported to be effective over 700 °C. Noble metal and Ni supported on Ce rich (Ce \geq 0.5) supports were effective in partial oxidation and autothermal reforming of methane and of oxygenated hydrocarbons. Conflicting results on Zr rich (Ce \leq 0.2) were also reported on both the processes. Only Ce rich (Ce \geq 0.5) supports were reported to be effective in dry reforming of methane. Addition of Zr to Ce to form Ce–ZrO₂ solid solutions have shown to improve the performance of ceria as a support in hydrogen production. But redox capability, OSC, surface area, and thermal resistance of the material are not yet suitable for long term application and commercialization. Addition of Al₂O₃ to Ce–ZrO₂ was shown to improve the properties of Ce–ZrO₂ solid solution and help in cost reduction.

In case of alumina modified Ce–ZrO₂ catalyst, the Zr rich (Ce \leq 0.2) catalyst was shown to be effective in steam reforming and dry reforming of methane. In autothermal reforming of methane and ethanol, alumina modified by Ce rich (Ce \geq 0.5) supports were shown to be effective, along with partial oxidation of methane.

Acknowledgment

The authors wish to acknowledge the [Research Councils UK](#) for funding in sustainable hydrogen production (EP/G01244X/1).

Appendix A

The definitions used by various authors are listed below.

A.1 Hydrogen yield definitions

Biswas and Kunzru [19] along with Roh et al. [60] defined hydrogen yield in SRE is as below.

$$Y_{H_2} = \left[\frac{(\text{mol}_{H_2})}{(\text{mol}_{C_2H_5OH})} \right] \quad \text{Eqn 17}$$

Dave and Pant [21] defined the yield of hydrogen in SRG as below.

$$Y_{H_2} = \left[\frac{(\text{mol}_{H_2})}{(\text{mol}_{C_3H_8O_3})} \right] \quad \text{Eqn 18}$$

Laosiripojana et al. [55] defined hydrogen yield in SR and PO of PFAD as below.

$$Y_{H_2} (\%) = \left[\frac{(\%H_2)}{(2(\%CH_4) + 3(\%C_2H_6) + 2(\%C_2H_4))} \right] \times 100$$
$$Y_{H_2} (\%) = \left[\frac{(X_{H_2})}{(2(X_{CH_4}) + 3(X_{C_2H_6}) + 3(X_{C_3H_8}) + 2(C_2H_4))} \right] \times 100 \quad \text{Eqns 19 -20}$$

Lin et al. [58] defined hydrogen yield in SRE by the following equation.

$$Y_{H_2} (\%) = \left[\frac{(\text{mol}_{H_2})}{(\text{mol}_{C_2H_5OH} \times 6)} \right] \times 100 \quad \text{Eqn 21}$$

Roh et al. [46] defined hydrogen yield in SMR by Eq. (22).

$$Y_{H_2} (\%) = \left[\frac{(F_{H_2out})}{(3 \times F_{CH_4in})} \right] \times 100 \quad \text{Eqn 22}$$

Vagia and Lemonidou [65] defined hydrogen yield along with Yan et al. [54] and Zheng et al. [66] who defined hydrogen selectivity as below

$$Y_{H_2} (\%) = \left[\frac{(\text{mol}_{H_2})}{(\text{mol}_{CH_3COOH} \times 4)} \right] \times 100 \quad \text{Eqn 23}$$

Damyanova et al.[114] and Sukonket et al.[124] defined hydrogen yield in DRM as

$$Y_{H_2} (\%) = \left[\frac{(F_{H_2out})}{(F_{CH_4in})} \times \frac{1}{2} \right] \times 100 \quad \text{Eqn 24}$$

A.2 Hydrogen selectivity definitions

Dave and Pant [21] reported hydrogen selectivity as below

$$S_{H_2} (\%) = \left[\frac{(F_{H_2 \text{out}})}{(\text{C atom in gas phase})} \times \frac{1}{RR} \right] \times 100$$

Eqn 25

Cao et al. [71] defined hydrogen selectivity by the following definition.

$$S_{H_2} (\%) = \left[\frac{(n_{H_2 \text{ produced}})}{((n_{H_2O \text{ converted}}) + (2n_{CH_4 \text{ converted}}))} \right] \times 100$$

$$n_{H_2O \text{ (converted)}} = (n_{CO \text{ produced}} + 2 \times n_{CO_2 \text{ produced}}) - (2 \times n_{O_2 \text{ consumed}})$$

Eqn 26-27

Larrondo et al. [105] defined hydrogen selectivity as below.

$$S_{H_2} (\%) = \left[\frac{(n_{H_2 \text{out}})}{(2(n_{CH_4 \text{in}} - n_{CH_4 \text{out}}))} \right] \times 100$$

Eqn 28

Pengpanich et al. [104] defined hydrogen selectivity as below.

$$S_{H_2} (\%) = \left[\frac{(n_{H_2 \text{out}})}{(n_{H_2 \text{out}} + n_{H_2O \text{out}})} \right] \times 100$$

Eqn 29

Roh et al. [60] defined hydrogen selectivity by Eq. (30).

$$S_{H_2} (\%) = \left[\frac{(n_{H_2 \text{out}})}{(n_{H_2 \text{out}} + 2n_{CH_4 \text{out}})} \right] \times 100$$

Eqn 30

Sukonket et al. [124] defined hydrogen selectivity by Eq. (31).

$$S_{H_2} (\%) = \left[\frac{(F_{H_2 \text{out}})}{(F_{H_2 \text{out}})_{\text{from DRM}} + (n_{H_2 \text{out}})_{\text{from complete SRM}}} \right] \times 100$$

Eqn 31

Srisiriwat et al. [79] defined hydrogen selectivity by Eq. (32).

$$S_{H_2} (\%) = \frac{F_{i \text{out}}}{\sum_i F_{i \text{out}}} \times 100$$

Eqn 32

Where F_i is flow rate of species i at outlet of the reactor.

Youn et al. [69] defined hydrogen selectivity by Eq. (33).

$$S_{H_2} (\%) = \left[\frac{(n_{H_2})}{((n_{C_2H_5OH \text{in}} - n_{C_2H_5OH \text{out}}) + (n_{H_2O \text{in}} - n_{H_2O \text{out}}))} \right] \times 100$$

Eqn 33

Conversion and molar composition in all most all the evaluations are defined as below

$$X (\%) = \frac{(\text{hydrocarbon})_{\text{in}} - (\text{hydrocarbon})_{\text{out}}}{(\text{hydrocarbon})_{\text{in}}} \times 100$$

Eqn 34

For e.g. in case of methane and ethanol conversion is defined as below

$$X (\%) = \frac{(\text{methane})_{\text{in}} - (\text{methane})_{\text{out}}}{(\text{methane})_{\text{in}}} \times 100$$
 Eqn 35

$$X (\%) = \frac{(\text{ethanol})_{\text{in}} - (\text{ethanol})_{\text{out}}}{(\text{ethanol})_{\text{in}}} \times 100$$
 Eqn 36

Dave and Pant [21] defined conversion differently than the common conversion definition.

$$\text{Glycerol conversion } (\%) = \left[\frac{(\text{C atoms in gas phase})}{\text{carbon in feed}} \right] \times 100$$
 Eqn 37

$$M_p (\%) = \frac{\text{mol}_p}{\sum \text{mol}_{\text{sp}}} \times 100$$
 Eqn 38

where the moles of each product are given mol_p and mol_{sp} is the total moles of products.

While Abreu et al. [51] defined hydrogen molar composition as

$$M_p = \frac{\text{mol}_{\text{H}_2 \text{ produced}}}{\text{mol}_{\text{CH}_4 \text{ converted}}}$$
 Eqn 39

References

- [1] A. Trovarelli, C. de Leitenburg, M. Boaro and G. Dolcetti, The utilization of ceria in industrial catalysis, *Catal Today* **50**, 1999, 353–367.
- [2] L. Scott, D.M. Swartz, M.T. Seabaugh, C.J. Holt and W. Dawson, Fuel processing catalysts based on nanoscale ceria, *Fuel Cells Bull* **4**, 2001, 7–10.
- [3] M. O'Connell and M.A. Morris, New ceria-based catalysts for pollution abatement, *Catal Today* **59**, 2000, 387–393.
- [4] T.S. Stefanik and H.L. Tuller, Ceria-based gas sensors, *J Eur Ceram Soc* **21**, 2001, 1967–1970.
- [5] H. Inaba and H. Tagawa, Ceria-based solid electrolytes, *Solid State Ionics* **83**, 1996, 1–16.
- [6] J. Kaspar, P. Fornasiero and M. Graziani, Use of CeO₂-based oxides in the three-way catalysis, *Catal Today* **50**, 1999, 285–298.
- [7] J.L. Ayastuy, A. Gurbani, M.P. González-Marcos and M.A. Gutiérrez-Ortiz, Effect of copper loading on copper-ceria catalysts performance in CO selective oxidation for fuel cell applications, *Int J Hydrogen Energy* **35**, 2010, 1232–1244.
- [8] Q. Zhang, J. Wen, M. Shen and J. Wang, Effect of different mixing ways in palladium/ceria–zirconia/alumina preparation on partial oxidation of methane, *J Rare Earths* **26**, 2008, 700–704.
- [9] J. Lahaye, S. Boehm, P. Chambrion and P. Ehrburger, Influence of cerium oxide on the formation and oxidation of soot, *Combust Flame* **104**, 1996, 199–207.
- [10]

J.I. Gutiérrez-Ortiz, B. de Rivas, R. López-Fonseca and J.R. González-Velasco, Catalytic purification of waste gases containing VOC mixtures with Ce/Zr solid solutions, *Appl Catal B* **65**, 2006, 191–200.

[11]

G. Zhou and R.J. Gorte, Thermodynamic investigation of the redox properties for ceria-hafnia, ceria-terbia, and ceria-praseodymia solid solutions, *J Phys Chem B* **112**, 2008, 9869–9875.

[12]

S. Hilaire, X. Wang, T. Luo, R.J. Gorte and J. Wagner, A comparative study of water-gas-shift reaction over ceria-supported metallic catalysts, *Appl Catal A* **258**, 2004, 271–276.

[13]

C.A. Bernardo, I. Alstrup and J.R. Rostrup-Nielsen, Carbon deposition and methane steam reforming on silica-supported Ni–Cu catalysts, *J Catal* **96**, 1985, 517–534.

[14]

J. Xu, C.M.Y. Yeung, J. Ni, F. Meunier, N. Acerbi, M. Fowles, et al., Methane steam reforming for hydrogen production using low water-ratios without carbon formation over ceria coated Ni catalysts, *Appl Catal A* **345**, 2008, 119–127.

[15]

L. Pino, A. Vita, F. Cipiti, M. Laganà and V. Recupero, Performance of Pt/CeO₂ catalyst for propane oxidative steam reforming, *Appl Catal A* **306**, 2006, 68–77.

[16]

X. Wang and R.J. Gorte, A study of steam reforming of hydrocarbon fuels on Pd/ceria, *Appl Catal A* **224**, 2002, 209–218.

[17]

N. Laosiripojana and S. Assabumrungrat, Hydrogen production from steam and autothermal reforming of LPG over high surface area ceria, *J Power Sources* **158**, 2006, 1348–1357.

[18]

N. Laosiripojana and S. Assabumrungrat, Conversion of poisonous methanethiol to hydrogen-rich gas by chemisorption/reforming over nano-scale CeO₂: The use of CeO₂ as catalyst coating material, *Appl Catal B* **102**, 2011, 267–275.

[19]

P. Biswas and D. Kunzru, Steam reforming of ethanol for production of hydrogen over Ni/CeO–ZrO catalyst: Effect of support and metal loading, *Int J Hydrogen Energy* **32**, 2007, 969–980.

[20]

C. Pojanavaraphan, A. Luengnaruemitchai and E. Gulari, Effect of catalyst preparation on Au/Ce_{1-x}Zr_xO₂ and Au–Cu/Ce_{1-x}Zr_xO₂ for steam reforming of methanol, *Int J Hydrogen Energy* **38**, 2013, 1348–1362.

[21]

C.D. Dave and K.K. Pant, Renewable hydrogen generation by steam reforming of glycerol over zirconia promoted ceria supported catalyst, *Renew Energy* **36**, 2011, 3195–3202.

[22]

J. Kašpar, P. Fornasiero and N. Hickey, Automotive catalytic converters: current status and some perspectives, *Catal Today* **77**, 2003, 419–449.

[23]

N. Laosiripojana and S. Assabumrungrat, Methane steam reforming over Ni/Ce–ZrO₂ catalyst: Influences of Ce–ZrO₂ support on reactivity, resistance toward carbon formation, and intrinsic reaction kinetics, *Appl Catal A* **290**, 2005, 200–211.

[24]

N. Laosiripojana, D. Chadwick and S. Assabumrungrat, Effect of high surface area CeO₂ and Ce–ZrO₂ supports over Ni catalyst on CH₄ reforming with H₂O in the presence of O₂, H₂, and CO₂, *Chem Eng J* **138**, 2008, 264–273.

[25]

E. Aneggi, M. Boaro, C.D. Leitenburg, G. Dolcetti and A. Trovarelli, Insights into the redox properties of ceria-based oxides and their implications in catalysis, *J Alloys Compd* **408–412**, 2006, 1096–1102.

[26]

- S. Bernal, J.J. Calvino, M.A. Cauqui, J.M. Gatica, C. Larese, J.A. Pérez Omil, et al., Some recent results on metal/support interaction effects in NM/CeO₂ (NM: noble metal) catalysts, *Catal Today* **50**, 1999, 175–206.
- [27]
Y. Nagai, T. Yamamoto, T. Tanaka, S. Yoshida, T. Nonaka, T. Okamoto, et al., X-ray absorption fine structure analysis of local structure of CeO₂–ZrO₂ mixed oxides with the same composition ratio (Ce/Zr=1), *Catal Today* **74**, 2002, 225–234.
- [28]
Z. Yang, Q. Wang and S. Wei, The effect of Zr-doping on the interaction of water molecules with the ceria (111) surface, *Surf Sci* **605**, 2011, 351–360.
- [29]
E. Aneggi, C. de Leitenburg, J. Llorca and A. Trovarelli, Higher activity of Diesel soot oxidation over polycrystalline ceria and ceria–zirconia solid solutions from more reactive surface planes, *Catal Today* **197**, 2012, 119–126.
- [30]
E. Aneggi, M. Boaro, C.D. Leitenburg, G. Dolcetti and A. Trovarelli, Insights into the redox properties of ceria-based oxides and their implications in catalysis, *J Alloys Compd* **408–412**, 2006, 1096–1102.
- [31]
A. Pappacena, K. Schermanz, A. Sagar, E. Aneggi and A. Trovarelli, Development of a modified co-precipitation route for thermally resistant, high surface area ceria–zirconia based solid solutions, In: E.M. Gaigneaux MDSHPAJJAM and P. Ruiz, (Eds.), *Studies in Surface Science and Catalysis*, 2010, Elsevier, 835–838.
- [32]
A. Trovarelli, M. Boaro, E. Rocchini, C. de Leitenburg and G. Dolcetti, Some recent developments in the characterization of ceria-based catalysts, *J Alloys Compd* **323–324**, 2001, 584–591.
- [33]
G. Vlaic, P. Fornasiero, S. Geremia, J. Kaspar and M. Graziani, Relationship between the zirconia-promoted reduction in the Rh-loaded Ce_{0.5}Zr_{0.5}O₂ mixed oxide and the Zr–O Local Structure, *J Catal* **168**, 1997, 386–392.
- [34]
P. Fornasiero, G. Balducci, R. Di Monte, J. Kaspar, V. Sergo, G. Gubitosa, et al., Modification of the redox behavior of CeO₂ Induced by structural doping with ZrO₂, *J Catal* **164**, 1996, 173–183.
- [35]
M.H. Yao, R.J. Baird, F.W. Kunz and T.E. Hoost, An XRD and TEM investigation of the structure of alumina-supported ceria–zirconia, *J Catal* **166**, 1997, 67–74.
- [36]
X. Karatzas, K. Jansson, A. González, J. Dawody and L.J. Pettersson, Autothermal reforming of low-sulfur diesel over bimetallic RhPt supported on Al₂O₃, CeO₂–ZrO₂, SiO₂ and TiO₂, *Appl Catal B* **106**, 2011, 476–487.
- [37]
S. Lemaux, A. Bensaddik, A.M.J. van der Eerden, J.H. Bitter and D.C. Koningsberger, Understanding of enhanced oxygen storage capacity in Ce_{0.5}Zr_{0.5}O₂; the presence of an anharmonic pair distribution function in the Zr–O₂ subshell as analyzed by XAFS spectroscopy, *J Phys Chem B* **105**, 2001, 4810–4815.
- [38]
P. Fornasiero, E. Fonda, R. Di Monte, G. Vlaic, J. Kaspar and M. Graziani, Relationships between structural/textural properties and redox behavior in Ce_{0.6}Zr_{0.4}O₂ mixed oxides, *J Catal* **187**, 1999, 177–185.
- [39]
A. Trovarelli, F. Zamar, J. Llorca, Cd Leitenburg, G. Dolcetti and J.T. Kiss, Nanophase fluorite-structured CeO₂–ZrO₂ catalysts prepared by high-energy mechanical milling, *J Catal* **169**, 1997, 490–502.
- [40]
J. Fan, X. Wu, R. Ran and D. Weng, Influence of the oxidative/reductive treatments on the activity of Pt/Ce_{0.67}Zr_{0.33}O₂ catalyst, *Appl Surf Sci* **245**, 2005, 162–171.
- [41]

- X. Wu, J. Fan, R. Ran and D. Weng, Effect of preparation methods on the structure and redox behavior of platinum–ceria–zirconia catalysts, *Chem Eng J* **109**, 2005, 133–139.
[42]
- S. Ahmed and M. Krumpelt, Hydrogen from hydrocarbon fuels for fuel cells, *Int J Hydrogen Energy* **26**, 2001, 291–301.
[43]
- M.A. Penã, J.P. Gómez and J.L.G. Fierro, New catalytic routes for syngas and hydrogen production, *Appl Catal A* **144**, 1996, 7–57.
[44]
- A. Platon, H.-S. Roh, D. King and Y. Wang, Deactivation studies of Rh/Ce_{0.8}Zr_{0.2}O₂ catalysts in low temperature ethanol steam reforming, *Top Catal* **46**, 2007, 374–379.
[45]
- K. Kusakabe, K.-I. Sotowa, T. Eda and Y. Iwamoto, Methane steam reforming over Ce–ZrO₂-supported noble metal catalysts at low temperature, *Fuel Process Technol* **86**, 2004, 319–326.
[46]
- H.-S. Roh, K.-W. Jun, W.-S. Dong, J.-S. Chang, S.-E. Park and Y.-I. Joe, Highly active and stable Ni/Ce–ZrO₂ catalyst for H₂ production from methane, *J Mol Catal A: Chem* **181**, 2002, 137–142.
[47]
- H.-S. Roh, I.-H. Eum and D.-W. Jeong, Low temperature steam reforming of methane over Ni–Ce(1–x)Zr(x)O₂ catalysts under severe conditions, *Renew Energy* **42**, 2012, 212–216.
[48]
- H.-S. Roh, K.Y. Koo and W.L. Yoon, Combined reforming of methane over co-precipitated Ni–CeO₂, Ni–ZrO₂ and Ni–Ce_{0.8}Zr_{0.2}O₂ catalysts to produce synthesis gas for gas to liquid (GTL) process, *Catal Today* **146**, 2009, 71–75.
[49]
- W.-S. Dong, H.-S. Roh, K.-W. Jun, S.-E. Park and Y.-S. Oh, Methane reforming over Ni/Ce–ZrO₂ catalysts: effect of nickel content, *Appl Catal A* **226**, 2002, 63–72.
[50]
- H.-S. Roh, K.-W. Jun and S.-E. Park, Methane-reforming reactions over Ni/Ce–ZrO₂/θ-Al₂O₃ catalysts, *Appl Catal A* **251**, 2003, 275–283.
[51]
- A.J. de Abreu, A.F. Lucrédio and E.M. Assaf, Ni catalyst on mixed support of CeO₂–ZrO₂ and Al₂O₃: Effect of composition of CeO₂–ZrO₂ solid solution on the methane steam reforming reaction, *Fuel Process Technol* **102**, 2012, 140–145.
[52]
- D. Srinivas, C.V.V. Satyanarayana, H.S. Potdar and P. Ratnasamy, Structural studies on NiO–CeO₂–ZrO₂ catalysts for steam reforming of ethanol, *Appl Catal A* **246**, 2003, 323–334.
[53]
- J. Ye, Y. Wang and Y. Liu, NiO–Ce_{0.5}Zr_{0.5}O₂ catalysts prepared by citric acid method for steam reforming of ethanol, *J Rare Earths* **26**, 2008, 831–835.
[54]
- C.-F. Yan, F.-F. Cheng and R.-R. Hu, Hydrogen production from catalytic steam reforming of bio-oil aqueous fraction over Ni/CeO₂–ZrO₂ catalysts, *Int J Hydrogen Energy* **35**, 2010, 11693–11699.
[55]
- N. Laosiripojana, W. Kiatkittipong, S. Charojrochkul and S. Assabumrungrat, Effects of support and co-fed elements on steam reforming of palm fatty acid distillate (PFAD) over Rh-based catalysts, *Appl Catal A* **383**, 2010, 50–57.
[56]
- A. Shotipruk, S. Assabumrungrat, P. Pavasant and N. Laosiripojana, Reactivity of CeO₂ and Ce–ZrO₂ toward steam reforming of palm fatty acid distilled (PFAD) with co-fed oxygen and hydrogen, *Chem Eng Sci* **64**, 2009, 459–466.
[57]
- H. Oguchi, T. Nishiguchi, T. Matsumoto, H. Kanai, K. Utani, Y. Matsumura, et al., Steam reforming of methanol over Cu/CeO₂/ZrO₂ catalysts, *Appl Catal A* **281**, 2005, 69–73.
[58]

- S.S.Y. Lin, H. Daimon and S.Y. Ha, Co/CeO₂-ZrO₂ catalysts prepared by impregnation and coprecipitation for ethanol steam reforming, *Appl Catal A* **366**, 2009, 252-261. [59]
- T.A. Maia, J.M. Assaf and E.M. Assaf, Steam reforming of ethanol for hydrogen production on Co/CeO₂-ZrO₂ catalysts prepared by polymerization method, *Mater Chem Phys* **132**, 2012, 1029-1034. [60]
- H.-S. Roh, Y. Wang and D. King, Selective production of hydrogen from ethanol at low temperatures over Rh/ZrO₂-CeO₂; Catalysts, *Top Catal* **49**, 2008, 32-37. [61]
- H.-S. Roh, A. Platon, Y. Wang and D. King, Catalyst deactivation and regeneration in low temperature ethanol steam reforming with Rh/CeO₂-ZrO₂ catalysts, *Catal Lett* **110**, 2006, 1-6. [62]
- H.-S. Roh, Y. Wang, D. King, A. Platon and Y.-H. Chin, Low temperature and H₂ selective catalysts for ethanol steam reforming, *Catal Lett* **108**, 2006, 15-19. [63]
- S.M. de Lima, A.M. Silva, I.O. da Cruz, G. Jacobs, B.H. Davis, L.V. Mattos, et al., H₂ production through steam reforming of ethanol over Pt/ZrO₂, Pt/CeO₂ and Pt/CeZrO₂ catalysts, *Catal Today* **138**, 2008, 162-168. [64]
- A. Birot, F. Epron, C. Descorme and D. Duprez, Ethanol steam reforming over Rh/Ce_xZr_{1-x}O₂ catalysts: impact of the CO-CO₂-CH₄ interconversion reactions on the H₂ production, *Appl Catal B* **79**, 2008, 17-25. [65]
- E.C. Vagia and A.A. Lemonidou, Investigations on the properties of ceria-zirconia-supported Ni and Rh catalysts and their performance in acetic acid steam reforming, *J Catal* **269**, 2010, 388-396. [66]
- X.-x. Zheng, C.-f. Yan, R.-r. Hu, J. Li, H. Hai, W.-m. Luo, et al., Hydrogen from acetic acid as the model compound of biomass fast-pyralysis oil over Ni catalyst supported on ceria-zirconia, *Int J Hydrogen Energy* **37**, 2012, 12987-12993. [67]
- Hu R-r, Yan C-f, Zheng X-x, Liu H, Zhou Z-y. Carbon deposition on Ni/ZrO₂-CeO₂ catalyst during steam reforming of acetic acid. *Int J Hydrogen Energy*. [68]
- H.-S. Roh, K.-W. Jun, W.-S. Dong, S.-E. Park and Y.-S. Baek, Highly stable Ni catalyst supported on Ce-ZrO₂ for oxy-steam reforming of methane, *Catal Lett* **74**, 2001, 31-36. [69]
- M.H. Youn, J.G. Seo, K.M. Cho, S. Park, D.R. Park, J.C. Jung, et al., Hydrogen production by auto-thermal reforming of ethanol over nickel catalysts supported on Ce-modified mesoporous zirconia: Effect of Ce/Zr molar ratio, *Int J Hydrogen Energy* **33**, 2008, 5052-5059. [70]
- P. Biswas and D. Kunzru, Oxidative steam reforming of ethanol over Ni/CeO₂-ZrO₂ catalyst, *Chem Eng J* **136**, 2008, 41-49. [71]
- L. Cao, L. Pan, C. Ni, Z. Yuan and S. Wang, Autothermal reforming of methane over Rh/Ce_{0.5}Zr_{0.5}O₂ catalyst: effects of the crystal structure of the supports, *Fuel Process Technol* **91**, 2010, 306-312. [72]
- J.A.C. Ruiz, F.B. Passos, J.M.C. Bueno, E.F. Souza-Aguiar, L.V. Mattos and F.B. Noronha, Syngas production by autothermal reforming of methane on supported platinum catalysts, *Appl Catal A* **334**, 2008, 259-267. [73]
- J.S. Lisboa, L.E. Terra, P.R.J. Silva, H. Saitovitch and F.B. Passos, Investigation of Ni/Ce-ZrO₂ catalysts in the autothermal reforming of methane, *Fuel Process Technol* **92**, 2011, 2075-2082. [74]

- S.C. Dantas, J.C. Escritori, R.R. Soares and C.E. Hori, Effect of different promoters on Ni/CeZrO₂ catalyst for autothermal reforming and partial oxidation of methane, *Chem Eng J* **156**, 2010, 380–387.
- [75]
J.C. Escritori, S.C. Dantas, R.R. Soares and C.E. Hori, Methane autothermal reforming on nickel–ceria–zirconia based catalysts, *Catal Commun* **10**, 2009, 1090–1094.
- [76]
X. Cai, X. Dong and W. Lin, Autothermal reforming of methane over Ni catalysts supported on CuO–ZrO₂–CeO₂–Al₂O₃, *J Nat Gas Chem* **15**, 2006, 122–126.
- [77]
S.M. de Lima, I.O. da Cruz, G. Jacobs, B.H. Davis, L.V. Mattos and F.B. Noronha, Steam reforming, partial oxidation, and oxidative steam reforming of ethanol over Pt/CeZrO₂ catalyst, *J Catal* **257**, 2008, 356–368.
- [78]
W. Cai, P.R. Piscina, K. Gabrowska and N. Homs, Hydrogen production from oxidative steam reforming of bio-butanol over CoIr-based catalysts: Effect of the support, *Bioresour Technol* **128**, 2013, 467–471.
- [79]
N. Srisiriwat, S. Therdthianwong and A. Therdthianwong, Oxidative steam reforming of ethanol over Ni/Al₂O₃ catalysts promoted by CeO₂, ZrO₂ and CeO₂–ZrO₂, *Int J Hydrogen Energy* **34**, 2009, 2224–2234.
- [80]
K. Kamonsuangkasem, S. Therdthianwong and A. Therdthianwong, Hydrogen production from yellow glycerol via catalytic oxidative steam reforming, *Fuel Process Technol* **106**, 2013, 695–703.
- [81]
M.D. Salazar-Villalpando, D.A. Berry and T.H. Gardner, Partial oxidation of methane over Rh/supported-ceria catalysts: effect of catalyst reducibility and redox cycles, *Int J Hydrogen Energy* **33**, 2008, 2695–2703.
- [82]
M.D. Salazar-Villalpando and A.C. Miller, Hydrogen production by methane decomposition and catalytic partial oxidation of methane over Pt/Ce_xGd_{1-x}O₂ and Pt/Ce_xZr_{1-x}O₂, *Chem Eng J* **166**, 2011, 738–743.
- [83]
M.D. Salazar-Villalpando and B. Reyes, Hydrogen production over Ni/ceria-supported catalysts by partial oxidation of methane, *Int J Hydrogen Energy* **34**, 2009, 9723–9729.
- [84]
A.S. Larimi and S.M. Alavi, Ceria–zirconia supported Ni catalysts for partial oxidation of methane to synthesis gas, *Fuel* **102**, 2012, 366–371.
- [85]
F.d.A. Silva, J.A.C. Ruiz, K.R. de Souza, J.M.C. Bueno, L.V. Mattos, F.B. Noronha, et al., Partial oxidation of methane on Pt catalysts: effect of the presence of ceria–zirconia mixed oxide and of metal content, *Appl Catal A* **364**, 2009, 122–129.
- [86]
P.P. Silva, F.A. Silva, H.P. Souza, A.G. Lobo, L.V. Mattos, F.B. Noronha, et al., Partial oxidation of methane using Pt/CeZrO₂/Al₂O₃ catalysts – effect of preparation methods, *Catal Today* **101**, 2005, 31–37.
- [87]
M.D. Salazar-Villalpando, D.A. Berry and A. Cugini, Role of lattice oxygen in the partial oxidation of methane over Rh/zirconia-doped ceria. Isotopic studies, *Int J Hydrogen Energy* **35**, 2010, 1998–2003. [88]
- F.B. Passos, E.R. de Oliveira, L.V. Mattos and F.B. Noronha, Partial oxidation of methane to synthesis gas on Pt/Ce_xZr_{1-x}O₂ catalysts: the effect of the support reducibility and of the metal dispersion on the stability of the catalysts, *Catal Today* **101**, 2005, 23–30.
- [89]
L.V. Mattos, E.R. de Oliveira, P.D. Resende, F.B. Noronha and F.B. Passos, Partial oxidation of methane on Pt/Ce–ZrO₂ catalysts, *Catal Today* **77**, 2002, 245–256.

[90]

L.V. Mattos, E. Rodino, D.E. Resasco, F.B. Passos and F.B. Noronha, Partial oxidation and CO₂ reforming of methane on Pt/Al₂O₃, Pt/ZrO₂, and Pt/Ce–ZrO₂ catalysts, *Fuel Process Technol* **83**, 2003, 147–161.

[91]

S. Fangli, S. Meiqing, F. Yanan, W. Jun and W. Duan, Influence of supports on catalytic performance and carbon deposition of palladium catalyst for methane partial oxidation, *J Rare Earths* **25**, 2007, 316–320.

[92]

R. Lanza, S.G. Järås and P. Canu, Partial oxidation of methane over supported ruthenium catalysts, *Appl Catal A* **325**, 2007, 57–67.

[93]

P.P. Silva, F. de A Silva, A.G. Lobo, H.P. de Souza, F.B. Passos, C.E. Hori, et al., Synthesis gas production by partial oxidation of methane on Pt/Al₂O₃, Pt/Ce–ZrO₂ and Pt/Ce–ZrO₂/Al₂O₃ catalysts, In: B. Xinhe and X. Yide, (Eds.), *Studies in Surface Science and Catalysis*, 2004, Elsevier, 157–162.

[94]

P.P. Silva, F.A. Silva, L.S. Portela, L.V. Mattos, F.B. Noronha and C.E. Hori, Effect of Ce/Zr ratio on the performance of Pt/CeZrO₂/Al₂O₃ catalysts for methane partial oxidation, *Catal Today* **107–108**, 2005, 734–740.

[95]

F.A. Silva, D.S. Martinez, J.A.C. Ruiz, L.V. Mattos, C.E. Hori and F.B. Noronha, The effect of the use of cerium-doped alumina on the performance of Pt/CeO₂/Al₂O₃ and Pt/CeZrO₂/Al₂O₃ catalysts on the partial oxidation of methane, *Appl Catal A* **335**, 2008, 145–152.

[96]

F.A. Silva, K.A. Resende, A.M. da Silva, K.R. de Souza, L.V. Mattos, M. Montes, et al., Syngas production by partial oxidation of methane over Pt/CeZrO₂/Al₂O₃ catalysts, *Catal Today* **180**, 2012, 111–116.

[97]

V.B. Mortola, J.A.C. Ruiz, L.V. Mattos, F.B. Noronha and C.E. Hori, Partial oxidation of methane using Pt/CeZrO₂/Al₂O₃ catalyst – effect of the thermal treatment of the support, *Catal Today* **133–135**, 2008, 906–912.

[98]

S. Boullosa-Eiras, T. Zhao, E. Vanhaecke, D. Chen and A. Holmen, Partial oxidation of methane to synthesis gas on Rh/ZrxCe_{1-x}O₂–Al₂O₃, *Catal Today* **178**, 2011, 12–24.

[99]

S. Boullosa-Eiras, T. Zhao, D. Chen and A. Holmen, Effect of the preparation methods and alumina nanoparticles on the catalytic performance of Rh/ZrxCe_{1-x}O₂–Al₂O₃ in methane partial oxidation, *Catal Today* **171**, 2011, 104–115.

[100]

Q. Zhang, M. Shen, J. Wen, J. Wang and Y. Fei, Partial oxidation of methane on Ni/CeO₂–ZrO₂/γ-Al₂O₃ prepared using different processes, *J Rare Earths* **26**, 2008, 347–351.

[101]

W.-S. Dong, K.-W. Jun, H.-S. Roh, Z.-W. Liu and S.-E. Park, Comparative study on partial oxidation of methane over Ni/ZrO₂, Ni/CeO₂ and Ni/Ce–ZrO₂ catalysts, *Catal Lett* **78**, 2002, 215–222.

[102] H.-S. Roh, W.-S. Dong, K.-W. Jun and S.-E. Park, Partial oxidation of methane over Ni catalysts supported on Ce–ZrO₂ mixed oxide, *Chem Lett* **30**, 2001, 88–89.

[103]

S. Xu and X. Wang, Highly active and coking resistant Ni/CeO₂–ZrO₂ catalyst for partial oxidation of methane, *Fuel* **84**, 2005, 563–567.

[104]

S. Pengpanich, V. Meeyoo and T. Rirksomboon, Methane partial oxidation over Ni/CeO₂–ZrO₂ mixed oxide solid solution catalysts, *Catal Today* **93–95**, 2004, 95–105.

[105]

- S.A. Larrondo, A. Kodjaian, I. Fábregas, M.G. Zimicz, D.G. Lamas, B.E. Walsøe de Reca, et al., Methane partial oxidation using Ni/Ce_{0.9}Zr_{0.1}O₂ catalysts, *Int J Hydrogen Energy* **33**, 2008, 3607–3613.
- [106]
L.V. Mattos and F.B. Noronha, Partial oxidation of ethanol on supported Pt catalysts, *J Power Sources* **145**, 2005, 10–15.
- [107]
W. Wang, C. Su, T. Zheng, M. Liao and Z. Shao, Nickel zirconia cerate cermet for catalytic partial oxidation of ethanol in a solid oxide fuel cell system, *Int J Hydrogen Energy* **37**, 2012, 8603–8612.
- [108]
N. Laosiripojana, W. Kiatkittipong and S. Assabumrungrat, Partial oxidation of palm fatty acids over Ce–ZrO₂: roles of catalyst surface area, lattice oxygen capacity and mobility, *AIChE J* **57**, 2011, 2861–2869.
- [109]
T. Odedairo, J. Chen and Z. Zhu, Metal-support interface of a novel Ni–CeO₂ catalyst for dry reforming of methane, *Catal Commun* **31**, 2013, 25–31.
- [110]
P. Djinović, Črnivec I.G. Osojnik, B. Erjavec and A. Pintar, Influence of active metal loading and oxygen mobility on coke-free dry reforming of Ni–Co bimetallic catalysts, *Appl Catal B* **125**, 2012, 259–270.
- [111]
X. Lv, J.-F. Chen, Y. Tan and Y. Zhang, A highly dispersed nickel supported catalyst for dry reforming of methane, *Catal Commun* **20**, 2012, 6–11.
- [112]
K. Nagaoka, K. Takanabe and K.-i. Aika, Modification of Co/TiO₂ for dry reforming of methane at 2 MPa by Pt, Ru or Ni, *Appl Catal A* **268**, 2004, 151–158.
- [113]
J. Ni, L. Chen, J. Lin and S. Kawi, Carbon deposition on borated alumina supported nano-sized Ni catalysts for dry reforming of CH₄, *Nano Energy* **1**, 2012, 674–686.
- [114]
S. Damyanova, B. Pawelec, K. Arishtirova, M.V.M. Huerta and J.L.G. Fierro, The effect of CeO₂ on the surface and catalytic properties of Pt/CeO₂–ZrO₂ catalysts for methane dry reforming, *Appl Catal B* **89**, 2009, 149–159.
- [115]
J. Chen, C. Yao, Y. Zhao and P. Jia, Synthesis gas production from dry reforming of methane over Ce_{0.75}Zr_{0.25}O₂-supported Ru catalysts, *Int J Hydrogen Energy* **35**, 2010, 1630–1642.
- [116]
H.S. Potdar, H.-S. Roh, K.-W. Jun, M. Ji and Z.-W. Liu, Carbon dioxide reforming of methane over co-precipitated Ni–Ce–ZrO₂ catalysts, *Catal Lett* **84**, 2002, 95–100.
- [117]
H.-S. Roh, H.S. Potdar, K.-W. Jun, J.-W. Kim and Y.-S. Oh, Carbon dioxide reforming of methane over Ni incorporated into Ce–ZrO₂ catalysts, *Appl Catal A* **276**, 2004, 231–239.
- [118]
H.-S. Roh, H.S. Potdar and K.-W. Jun, Carbon dioxide reforming of methane over co-precipitated Ni–CeO₂, Ni–ZrO₂ and Ni–Ce–ZrO₂ catalysts, *Catal Today* **93–95**, 2004, 39–44.
- [119]
K.-W. Jun, H.-S. Roh and K.R. Chary, Structure and catalytic properties of ceria-based nickel catalysts for CO₂ reforming of methane, *Catal Surv Asia* **11**, 2007, 97–113.
- [120]
H.-S. Roh, K.-W. Jun, S.-C. Baek and S.-E. Park, A Highly active and stable catalyst for carbon dioxide reforming of methane: Ni/Ce–ZrO₂/θ-Al₂O₃, *Catal Lett* **81**, 2002, 147–151.
- [121]
Jang W-J, Jeong D-W, Shim J-O, Roh H-S, Son IH, Lee SJ. H₂ and CO production over a stable Ni–MgO–Ce_{0.8}Zr_{0.2}O₂ catalyst from CO₂ reforming of CH₄. *Int J Hydrogen Energy*.

[122]

N. Wang, W. Chu, L. Huang and T. Zhang, Effects of Ce/Zr ratio on the structure and performances of Co-Ce_{1-x}Zr_xO₂ catalysts for carbon dioxide reforming of methane, *J Nat Gas Chem* **19**, 2010, 117–122.

[123]

P. Kumar, Y. Sun and R.O. Idem, Nickel-based ceria, zirconia, and ceria–zirconia catalytic systems for low-temperature carbon dioxide reforming of methane, *Energy Fuels* **21**, 2007, 3113–3123.

[124]

T. Sukonket, A. Khan, B. Saha, H. Ibrahim, S. Tantayanon, P. Kumar, et al., Influence of the catalyst preparation method, surfactant amount, and steam on CO₂ reforming of CH₄ over 5Ni/Ce_{0.6}Zr_{0.4}O₂ catalysts, *Energy Fuels* **25**, 2011, 864–877.

[125]

J. Chen, Q. Wu, J. Zhang and J. Zhang, Effect of preparation methods on structure and performance of Ni/Ce_{0.75}Zr_{0.25}O₂ catalysts for CH₄–CO₂ reforming, *Fuel* **87**, 2008, 2901–2907.

[126]

A. Kambolis, H. Matralis, A. Trovarelli and C. Papadopoulou, Ni/CeO₂–ZrO₂ catalysts for the dry reforming of methane, *Appl Catal A* **377**, 2010, 16–26.

[127]

L. Xu, H. Song and L. Chou, Mesoporous nanocrystalline ceria–zirconia solid solutions supported nickel based catalysts for CO₂ reforming of CH₄, *Int J Hydrogen Energy* **37**, 2012, 18001–18020.

[128]

Črnivec I.G. Osojnik, P. Djinović, B. Erjavec and A. Pintar, Effect of synthesis parameters on morphology and activity of bimetallic catalysts in CO₂–CH₄ reforming, *Chem Eng J* **207–208**, 2012, 299–307.